THE AMERICAN MINERALOGIST
JOURNAL OF THE MINERALOGICAL SOCIETY OF AMERICA

Vol. 26 JANUARY, 1941 No. 1

HYDROTHERMAL FORMATION OF CLAY MINERALS IN THE LABORATORY, PART II

F. H. NORTON, *Division of Ceramics, Department of Metallurgy, Massachusetts Institute of Technology.*

ABSTRACT

The same materials reported on in the first part of this work were treated under higher pressures of CO_2 and water vapor in order to determine more completely the field of reaction. The results show good agreement with the previous work, but carry the contours up to higher concentrations of CO_2 where the reaction practically ceases. As before, end products were obtained closely approximating, but not exactly identical with, many of the natural clay minerals. The artificial product is less perfectly crystallized and shows some deviation both in x-ray pattern and thermal curve from the natural product. A few runs were made with stronger acids.

INTRODUCTION

The results presented here are a continuation of the experiments reported in 1939, where a percolating type of reaction chamber was used to break down some of the felspars.[1] Here the work is continued further by carrying the reactions out under higher pressures of CO_2, and runs were also made on some additional minerals outside of the feldspar class in order to give a broader picture of the stability relations in these minerals.

It should again be emphasized that the properties of the synthetic clay minerals produced in the laboratory do not in most cases show complete agreement with those of the corresponding natural minerals. The x-ray patterns may show exact agreement except for one or two lines which are weak or absent. The thermal curves of the laboratory product usually have peaks slightly lower in temperature than their natural counterpart. This lack of agreement is not surprising in view of the comparatively short time of formation which produces fine and imperfect crystallization. For these reasons it is difficult to make positive identifications of the end product in many cases, although the type of mineral is quite certain.

---

[1] Norton, F. H., Hydrothermal formation of clay minerals in the laboratory: *Am. Mineral.*, **24,** 1–17 (1939).

PREVIOUS WORK

As in the previous paper no detailed mention is made here of the synthesis of the clay minerals, as these can be found in the excellent paper by Morey and Ingerson.[2]

APPARATUS

The apparatus used here was the same as reported in the previous paper, except that two reaction chambers were made for higher pressure work from chrome-nickel steel. Except for the higher pressures no changes were made in the method of operation. In Table 1 are given the total pressures in the reaction chamber under various initial pressures of CO_2 and temperature. At the higher pressures these values are somewhat variable, and depend on the amount of filling of the chamber.

TABLE 1

CO_2 pressure at room temp.	250°C	275°C	300°C	325°C	350°C
0	560	860	1230	1720	2380
125	775	1087	1467	1967	2638
250	990	1313	1703	2215	2895
375	1205	1540	1940	2460	3154
500	1420	1765	2175	2710	3410
600		2250	2650	3200	
700		2750	3200	3750	
800		3450	3900	4400	
900		4400	4800	5300	

RAW MATERIALS

In general, the same raw materials were used as in the previous work, with the exception of the following minerals which were obtained from Ward's Natural Science Establishment and appeared to be of a high grade of purity:

Analcite, from Table Mountain, Colorado.
Scolecite, from Teigarhorn, Iceland.

---

[2] Morey, G. W., and Ingerson, E., The pneumatolytic and hydrothermal alteration and synthesis of silicates: *Paper No. 937, Geophysical Laboratory, Carnegie Inst. of Washington*, (1937).

Volcanic glass, from Wyoming.
Diopside, from Templeton, Quebec, Canada.
Pyrope (Garnet), from Meronitz, Bohemia.
Oligoclase, from Mitchell County, North Carolina.
Andesine, from Palmietfontein, Transvaal.
Labradorite, from near Nain, Labrador.
Bytownite, from Crystal Bay, Minnesota.
Anorthite, from Miakejima, Japan.

RATE OF CONVERSION OF ALBITE

In Table 2 there is shown the test results on the conversion of albite. It will be noticed that this is a comparatively stable mineral, and even under the most favorable conditions the conversion is by no means complete. The previous work is checked fairly closely, although a few small changes have been incorporated into the more recent values.

TABLE 2. CONVERSION OF ALBITE ($Na_2O \cdot Al_2O_3 \cdot 6SiO_2$)

Conditions		Product	% Conversion
Temp.	CO_2 Initial Pressure		
250°	250 lbs./in.^{2}	Quartz, Montmorillonite or Beidellite	5
250°	500		0
275°	250	Quartz, Montmorillonite or Beidellite	20
300°	250	Montmorillonite or Beidellite	30
300°	500	Quartz, Montmorillonite or Beidellite	20
300°	650	Montmorillonite or Beidellite	10
300°	800		0
300°	925		0
350°	250	Montmorillonite or Beidellite	5
350°	500	Montmorillonite or Beidellite	5

The end product produced by this reaction was previously stated to be beidellite, but our more recent work would indicate that it could also be montmorillonite. In Fig. 1 is shown *x*-ray patterns of this end product compared with both beidellite and montmorillonite.

The thermal curves of the end product show a relatively strong double peak at low temperatures, which is characteristic of montmorillonite. The small peak at 550° may be due to a small amount of diaspore which would not show in the *x*-ray pattern. In Fig. 2 are shown thermal curves of the end product and the thermal curve of montmorillonite, which unfortunately does not give very characteristic high temperature peaks.

In Fig. 3 are shown the rates of conversion for the various pressure and temperature conditions. It will be seen that the greatest conversion rate occurs at 300° and about 300 pounds initial pressure of CO_2. At the very high CO_2 pressures there was no conversion so that the field of reaction is practically completed.

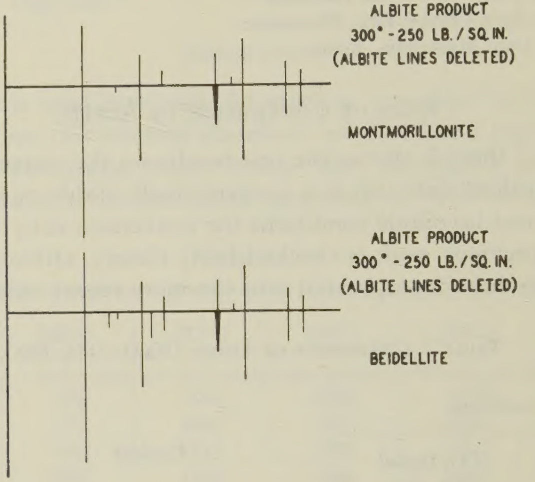

Fig. 1

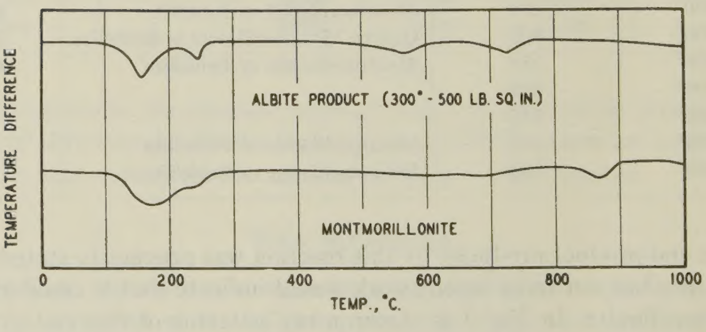

Fig 2

One run was made on fused albite and the end product seemed to be identical with that resulting from the crystalline material.

Rate of Conversion of Nephelite

In Table 3 is shown the conversion rates and end products for the various runs made on this material. Nephelite is fairly readily converted into an end product which checks closely with that of sericite, except in one case which was noted before, where the mineral gibbsite is indicated by the *x*-ray patterns. In Fig. 4, *x*-ray patterns of the reaction product from the run at 300°C. and a pressure of 375 pounds are compared with the pattern of natural sericite, showing excellent agreement. In Fig. 5 the pattern from the conversion product at 300° Centigrade and 500 pounds pressure is compared with sericite, and in Fig. 6 with gibbsite. It will be seen that both the patterns of sericite and gibbsite are well represented in this pattern.

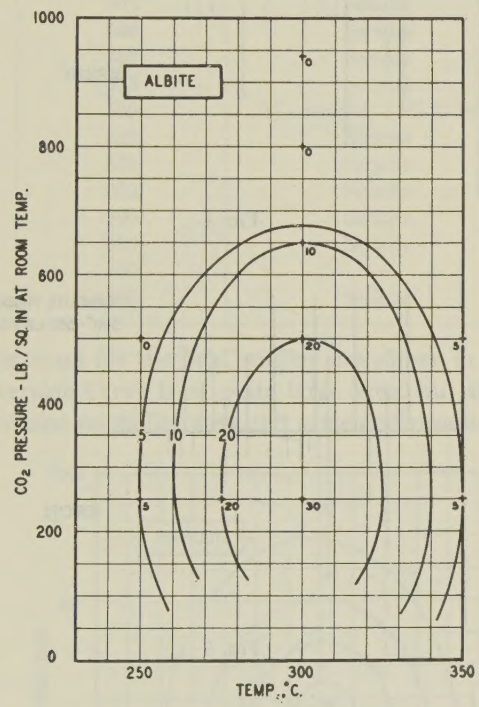

Fig. 3

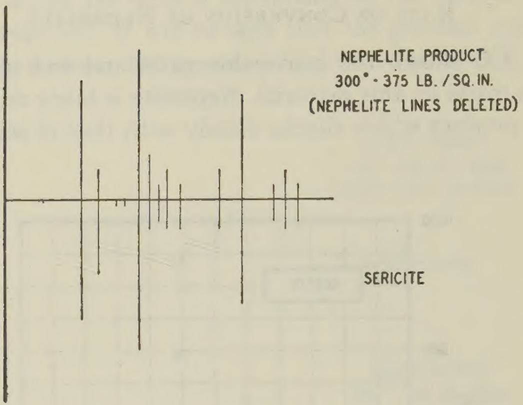

FIG. 4

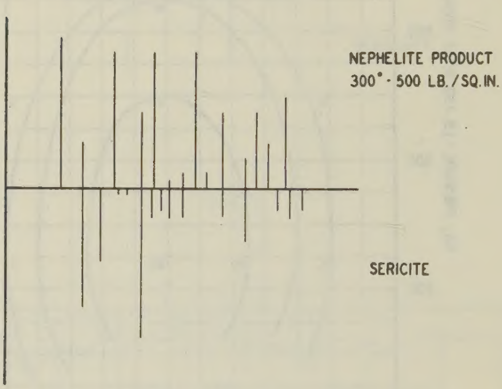

FIG. 5

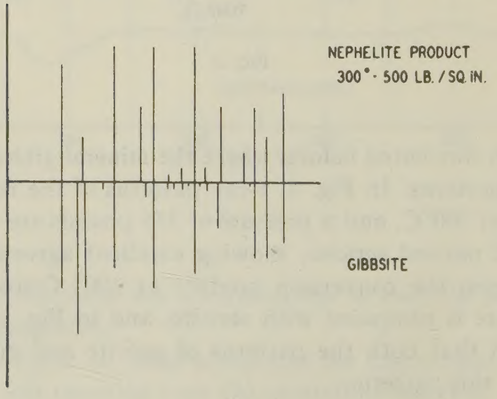

FIG. 6

TABLE 3. CONVERSION OF NEPHELITE ($Na_2O \cdot Al_2O_3 \cdot 2SiO_2$)

Conditions		Product	% Conversion
Temp.	CO_2 Pressure		
250°	500 lbs./in.^{2}	Sericite	20
275°	500	Sericite	60
275°	650	Sericite	50
300°	250	Sericite	70
300°	375	Sericite	80
300°	500	25% Sericite, 75% Gibbsite	100
300°	650	Sericite	90
300°	850	Sericite	30
300°	950	Sericite	10
325°	500	Sericite	60
325°	850	Sericite	10
350°	250	—	0
350°	500	Sericite	10

The reaction rates for the field studied are shown in Fig. 7, indicating that the conversion curve is of quite large area, but that the limits are well defined. Fused nephelite gave the same end product.

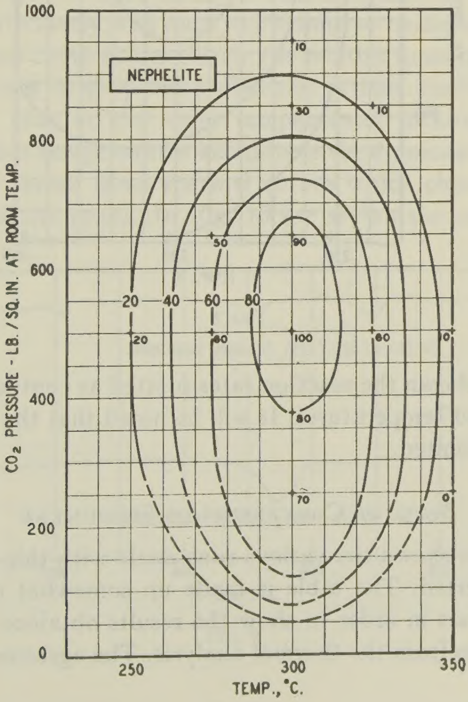

FIG. 7

Rate of Conversion of Orthoclase

In Table 4 are shown the various conditions to which this material was subjected. Here again the end product is sericite and the conditions under which the conversion occurs are rather limited. The results check well with our previous experiments, and the runs at higher pressure indicate no conversion. The *x*-ray and thermal curves of the reaction product are identical with the end product from nephelite.

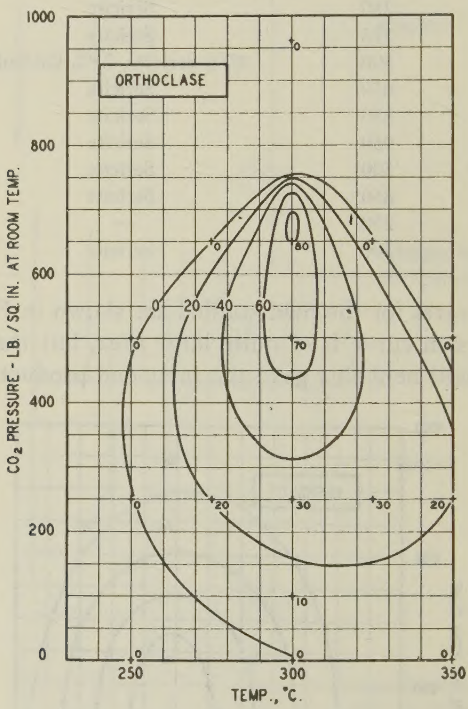

Fig. 8

In Fig. 8 are shown the reaction rates plotted as contours against various pressures and temperatures. It will be noted that the reaction area is comparatively limited.

Rate of Conversion of Spodumene

In Table 5 are shown the various runs made with this material, which is readily converted. The table is made up somewhat differently from the other minerals in order to show the results obtained from the *x*-ray analysis and also from the thermal analysis. The agreement between the

TABLE 4. CONVERSION OF ORTHOCLASE ($K_2O \cdot Al_2O_3 \cdot 6SiO_2$)

Conditions		Product	% Conversion
Temp.	CO_2 Pressure		
250°C	0 lbs./in.^{2}	—	0
250°	250	—	0
250°	500	—	0
275°	250	Sericite	20
275°	650	—	0
300°	0	—	0
300°	100	Sericite	10
300°	250	Sericite	30
300°	500	Sericite	70
300°	650	Sericite	80
300°	960	—	0
325°	250	Sericite	30
325°	650	—	0
350°	0	—	0
350°	250	Sericite	20
350°	500	—	0

two methods of analysis is not particularly close because the thermal method does not show inert minerals such as quartz or corundum, nor does it show particularly well montmorillonite or beidellite. On the other hand, the thermal curve shows clearly the relative amounts of kaolin and dickite, which vary in proportion with the various conditions of run. It will be noticed that at the lower temperatures dickite predominates, while at the higher temperatures kaolinite is the dominant material.

In Fig. 9 are shown some thermal curves which clearly indicate the dickite and kaolinite peaks. In Fig. 10 are shown the contours of total

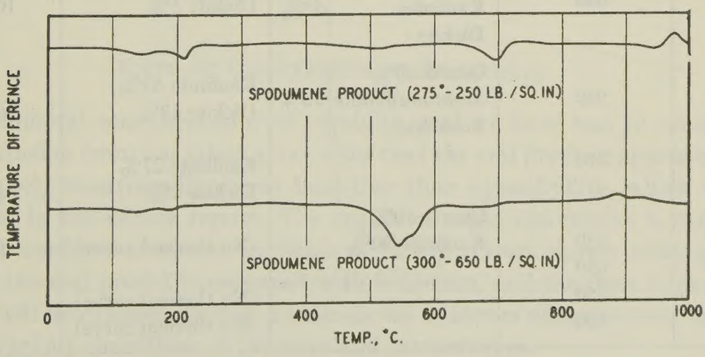

FIG. 9

TABLE 5. CONVERSION OF SPODUMENE ($Li_2O \cdot Al_2O_3 \cdot 4SiO_2$)

Conditions		Product and Approx. Amount		
Temp.	CO_2 Pressure	*X*-ray	Thermal Curve	% Total Conversion
250°	500 lbs./in.²	Quartz 25% Corundum 15%	Kaolinite 2% Dickite 18%	40
275°	250	Quartz 20% Montmorillonite Kaolinite } 80% Dickite	Kaolinite 11% Dickite 24%	100
275°	650	Quartz 25% Montmorillonite Kaolinite } 70% Dickite	Kaolinite 58% Dickite 15%	100
275°	850	Quartz 40% Montmorillonite Kaolinite } 60% Dickite	Kaolinite 22% Dickite 21%	100
300°	125	Quartz 10% Kaolinite } 90% Dickite	(No thermal curve)	100
300°	250	Quartz 10% Kaolinite } 90% Dickite	(No thermal curve)	100
300°	500	Quartz 10% Kaolinite } 90% Dickite	Kaolinite 113%	100
300°	650	Quartz 15% Montmorillonite Kaolinite } 85% Dickite	Kaolinite 82% Dickite 5%	100
300°	950	Quartz 30% Montmorillonite } 70% Beidellite	Kaolinite 53% Dickite 12%	100
300°	970	?	Kaolinite 27% Dickite 2%	40
325°	250	Quartz 10% Kaolinite 80%	(No thermal curve)	90
325°	650	—	—	0
350°	250		(No thermal curve)	0
350°	500		(No thermal curve)	0

conversion of spodumene, showing the comparatively large field in which the conversion is complete. In this case the contours are not completely closed at the high pressure side.

Fused spodumene gave the same end product as the original material.

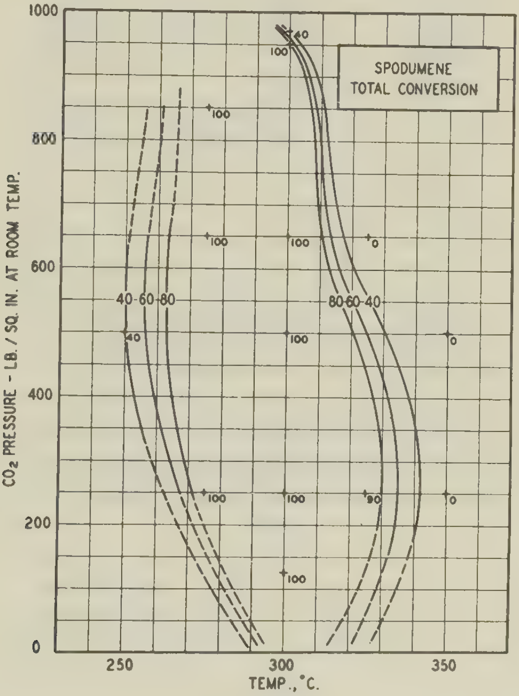

FIG. 10

RATE OF CONVERSION OF ANORTHITE

This mineral was checked over carefully, and we have had to come to the conclusion from our latest x-ray data that the end product approaches more closely montmorillonite or beidellite than pyrophyllite, which was indicated in the earlier report. The region of rapid conversion is rather narrowly confined as shown in Table 6. In Fig. 11 are shown x-ray patterns of the end product compared with beidellite, and the close approximation will be evident. In Fig. 12 are shown contours of conversion rates for the various conditions of pressure and temperature.

TABLE 6. CONVERSION OF ANORTHITE ($CaO \cdot Al_2O_3 \cdot 2SiO_2$)

Conditions		Product	% Conversion
Temp.	CO_2 Pressure		
250°	250 lbs./in.²	Montmorillonite or Beidellite	10
250°	500	Montmorillonite or Beidellite	10
275°	250	?	20
275°	650		0
300°	250	Montmorillonite or Beidellite	30
300°	500	Montmorillonite or Beidellite	70
300°	650		0
300°	850		0
300°	920		0
300°	950		0
325°	250	?	50
325°	650		0
350°	250	Montmorillonite or Beidellite (?)	30
350°	500		0

A sample of anorthite was fused and treated at 300° and 500 pounds of CO_2 pressure. The results indicated a product from the x-ray pattern of 20% kaolinite and 80% gibbsite. The kaolinite lines agree well with the standard material, but two strong lines of the gibbsite pattern were weak or missing. The thermal curves indicated dickite with some diaspore, as shown in Fig. 13.

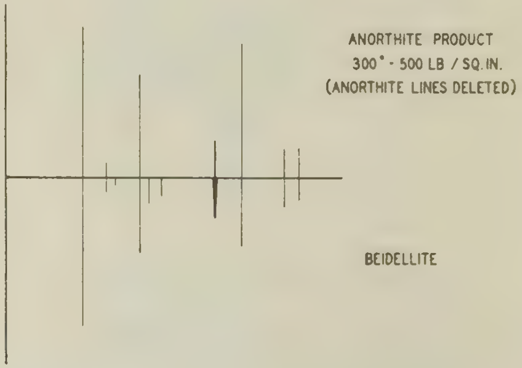

FIG. 11

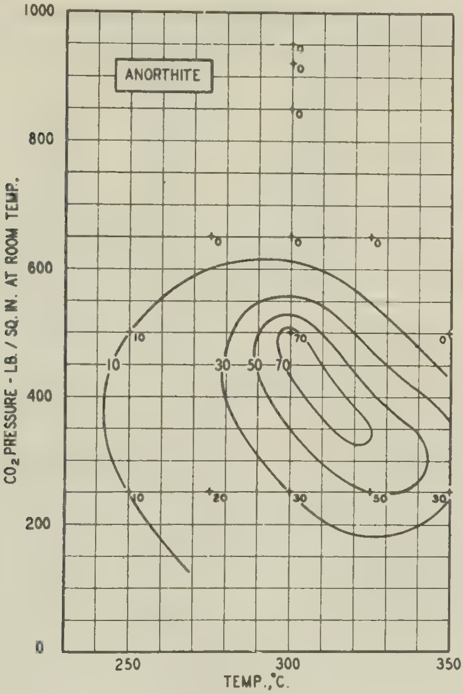

Fig. 12

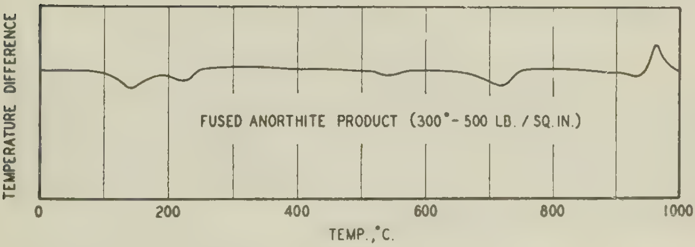

Fig. 13

Conversion of Other Minerals with Carbon Dioxide

In Table 7 are listed a number of other minerals which have been treated at a temperature and pressure which was believed to give the maximum rate of reaction, but as the general field was not covered we cannot be sure that some other temperature or pressure might not give a greater reaction rate.

The natural volcanic glass seemed to be converted quite readily under these conditions. The analysis of this material is:

SiO_2	74.7%
Al_2O_3	15.2%
K_2O	4.0 %
Na_2O	4.0 %
Fe_2O_3	1

TABLE 7. CONVERSION OF OTHER MINERALS

Parent Mineral	Formula	End Product	Temp.	Pres.	Conversion in 360 hrs.
Leucite	$K_2O \cdot Al_2O_3 \cdot 4SiO_2$	Sericite	300°C	500 lbs./in.^{2}	80
Petalite	$Li_2O \cdot Al_2O_3 \cdot 8SiO_2$	Kaolinite	300°	250	100
Petalite	$Li_2O \cdot Al_2O_3 \cdot 8SiO_2$	Quartz, Montmorillonite	300°	800	60
Lepidolite	$Li_2O \cdot 2Al_2O_3 \cdot K_2O \cdot 6SiO_2 \cdot 2H_2O$	Quartz	300°	500	Slight
Beryl	$3BeO \cdot Al_2O_3 \cdot 6SiO_2$	No change	300°	500	0
Pollucite	$2Cs_2O \cdot 2Al_2O_2 \cdot 9SiO_2 \cdot H_2O$	No change	300°	500	0
Kaolinite	$Al_2O_3 \cdot 2SiO_2 \cdot 2H_2O$	No change	300°	500	0
Analcite	$Na_2O \cdot Al_2O_3 \cdot 4SiO_2 \cdot 2H_2O$	Kaolinite Quartz, Dickite	300°	500	70
Scolecite	$CaO \cdot Al_2O_3 \cdot 3SiO_2 \cdot 3H_2O$	Sericite	300°	500	90
Nat. Volcanic Glass	—	Sericite Dickite	300°	500	50?

TREATMENT WITH STRONGER ACIDS

A few of the minerals were tested in the percolating reaction chamber with stronger acids, as shown in Table 8. It is rather interesting to note that in some cases the conversion with the stronger acids is not as rapid as with the carbon dioxide, a rather interesting fact when considering the formation of clay minerals in nature.

CHANGE IN RATE OF ALTERATION WITH DEPTH OF MATERIAL

In all of the preceding work, the sample for analysis of the treated material was taken from the top of the material in the reaction cup. In order to determine the change of the rate of reaction with depth, samples were taken from the top, middle, and bottom portions of the mass and subjected to x-ray and thermal analysis. Spodumene treated with water and CO_2 at 300° Centigrade and 650 lbs./in.^{2} was chosen for this treatment. The thermal analysis curves of the three parts of the reaction

TABLE 8. CONVERSION IN OTHER ACIDS

Mineral	Acid	Temp.	Product	% Conversion
Anorthite	.3N-HCl	300°C	—	None
Anorthite	.8N-HCl	300°	Montmorillonite	40
Albite	.8N-HCl	250°	—	Slight
Albite	.8N-HCl	300°	10% Quartz, 90% Kaolinite	100
Albite	.8N-HCl	350°	—	Slight
Orthoclase	.02N-HF	300°	—	None
Orthoclase	.01N-HCl	300°	—	None
Orthoclase	.3N-HCl	300°	—	None
Orthoclase	1N-H_2SO_4	300°	—	None
Pollucite	.8N-HCl	300°	Montmorillonite or Beidellite	70
Diopside	.8N-HCl	300°	—	None

product show the great difference in alteration between the top, the middle and bottom layers. The large double endothermic peak at 550° in the curve of the top layer is very small in the curve of the middle layer and is almost absent in the curve of the bottom layer. At the same time, the endothermic peak at 700° is barely discernible in the curve of the top layer and is very large in the curves of the middle and bottom layers. Assuming that the peak at 550° is due to kaolinite and that at 700° is due to dickite, the proportions of these minerals present in each layer is given in Table 9.

TABLE 9. SPODUMENE TREATED WITH H_2O AND CO_2 AT 300°C, 650 LBS./IN.^{2}

Position of Sample	Area of Peak at 550°	Area of Peak at 700°	% Kaolinite	% Dickite
Top	.37 in.^{2}	.02 in.^{2}	82	5
Middle	.05	.13	11	31
Bottom	.02	.15	4	36

Basis: 100% Kaolinite = .45 in.^{2}
100% Dickite = .42 in.^{2}

The *x*-ray patterns of the three layers do not show as good correlation as the thermal analysis curves; however they give good evidence that the reaction rate is not the same at all depths. The pattern of the top layer indicates that it is a mixture of quartz and an imperfectly formed kaolinite-dickite-montmorillonite mineral; the pattern of the middle layer corresponds to that of quartz with a small amount of montmorillonite; while the pattern of the bottom layer shows a mixture of 60% quartz and 40% montmorillonite. It is difficult to understand why the middle and bottom layers give very similar thermal curves yet show such different *x*-ray patterns.

Discussion of Results

Considering the results obtained in this investigation as a whole, it is evident that the rate of reaction in CO_2 charged water is a maximum in a rather limited region for most of the minerals, centered around 300° Centigrade and 500 pounds CO_2 pressure. Contrary to our original beliefs, the reaction rate in all cases seems to decrease at the very high pressures of CO_2, and in many cases the reaction becomes substantially zero at the higher acidity. These results, therefore, give us fairly definite limits as to the conditions under which reasonably rapid conversion can take place. However, it should not be concluded that in nature the clay minerals were all formed under these particular conditions as it is quite possible that the changes could go on outside of this region at rates so slow that they could not be detected in our laboratory experiments.

It will also be noted that the stability of the various minerals depends largely on an alkali content; that is, those minerals containing the largest percentage of alkali are the least stable.

There is also more evidence in this investigation than was shown previously that under certain conditions two end products can be formed at the same time. This was noted in the case of nephelite and spodumene, but the relative proportion of these products vary materially with the conditions of treatment.

It is interesting to notice how the reaction varies through the depth of the reacting material. In the one case illustrated there was a decided difference in the alteration product as we went from the top to the bottom of the charge. As might be expected, the amount of quartz was greater in the bottom than in the top, as this material evidentally is carried through by the percolating water in the form of more or less colloidal material.

In this investigation some runs were made with stronger acids and in several cases the reaction rate was lower than with CO_2 which indicates that the break up of the original minerals occurred more rapidly in weak acids than in strong ones under these conditions of temperature and pressure. This is a result somewhat contrary to that which we expected. On the other hand, pollucite, which showed no reaction with CO_2 under any conditions, reacted fairly rapidly in strong acid.

Conclusions

The conclusions drawn from this work are essentially the same as stated at the end of the previous report.

(1) Under the test conditions where CO_2-charged water is allowed to percolate through the finely ground mineral, a maximum reaction rate occurs at 300°C. and 500 lbs./sq. in. pressure.

(2) The end products, while similar to the various clay minerals are not identical with them in every respect.

(3) In most cases a single end product is formed, but under a few conditions two end products were formed simultaneously.

(4) In some cases strong acids did not show as high a conversion rate as carbonic acid.

Acknowledgments

This work has been made possible by the generosity of The Geological Society of America which has allotted funds to carry out this investigation. The author wishes to express his appreciation for this assistance. The careful laboratory work of Robert L. Green, and J. L. Hall who assisted with this problem, is gratefully acknowledged.

GEOMETRICAL CRYSTALLOGRAPHY OF PbO_2 AND Pb_5O_8

H. R. Davidson,

Department of Physics, Lehigh University.

Abstract

Large crystals of PbO_2 and Pb_5O_8 have been prepared by heating lead peroxide, sodium hydroxide, and water together in a steel bomb. The PbO_2 crystals so obtained are tetragonal ($c=0.6785$), twinning on (101), and show the forms: $\{101\}$, $\{111\}$, $\{211\}$, and $\{230\}$. Pb_5O_8 crystals are also tetragonal ($c=0.989$), twinning on (101). Crystals exhibit parallel growth on (110) and show the forms: $\{001\}$, $\{111\}$, $\{100\}$, and $\{110\}$. Some of the twin-crystals mimic hexagonal crystals.

During the preparation, for magnetic measurements, of specimens of intermediate oxides of lead by the method of Clark *et al.*,[1] and variants of it, several crystalline products other than those they have reported were obtained. Of particular interest were crossed acicular crystals which proved to be the elusive PbO_2. Large crystals of Pb_5O_8, adequate for goniometric study, were also obtained.

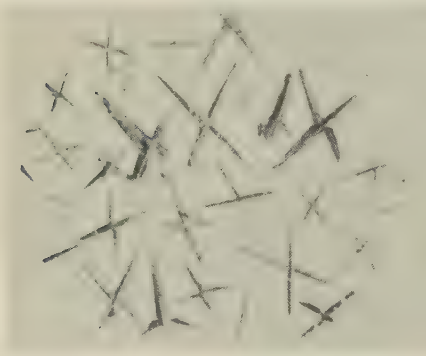

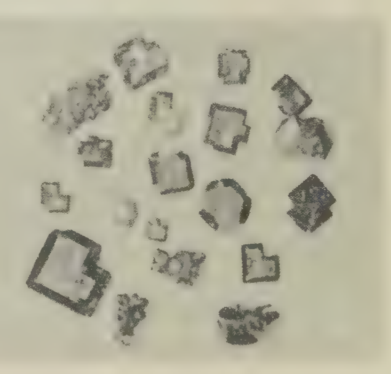

FIG. 1. Crystals of PbO_2. Magnification 6 diam.
FIG. 2. Crystals of Pb_6O_8. Magnification 6 diam.

The method employed in the production of these crystals consisted of heating sodium hydroxide, water, and lead peroxide together in a steel bomb which was very heavily gold plated over nickel, in order to prevent ferro-magnetic contamination. Heating was accomplished in an electric furnace whose temperature, determined by a chromel-alumel thermocouple, could be controlled accurately. One part of sodium hydroxide, four parts of water, and three parts of lead peroxide (0.0003% or less Mn) were held from four to six days in the bomb at a steady temperature between 260° and 390°C.

---

[1] Clark, G. L., Shieltz, N. C., Quirke, T. T., *Jour. Am. Chem. Soc.*, **59,** 2305-2308 (1937).

When the bomb was held at increasingly higher temperatures the degree of "reduction" of the PbO_2 became greater until, at the highest temperatures used, numerous flakes of yellow PbO were found mixed with the larger quantities of the higher oxides. Whether a simple removal of oxygen atoms from the PbO_2 crystal structure constitutes the reduction of PbO_2, or whether some essential intermediate product occurs is still problematical. Unsettled chemical questions, which need not be considered here, are involved:[2]

The goniometric measurement of the crystals so obtained presented certain difficulties. In the case of the Pb_5O_8 crystals, striations due to parallel growth caused most of the trouble. Faces of the form {001} in particular are so thoroughly striated on all measurable crystals that it was impossible to obtain a sharp signal. The pyramid faces are somewhat better, but none of them reflect a signal which could be measured with the desired precision. The most consistent results were obtained by measuring the angle between the normals to the (111) faces, thereby eliminating the highly striated (001) face.

In measuring the PbO_2 crystals the chief difficulty was caused by the minuteness of the pyramid faces. Although these crystals sometimes grow to a length of nearly 3 mm. their ends are usually mere points, as may be seen in Fig. 1. No normal signal was obtainable on any of the surfaces, but because of the small size of the pyramid faces it was possible to use a "pin-hole" image in measuring the angles.[3]

[2] Le Blanc and Eberius (*Zeits. physik. Chem.*, **A 160**, 69, 1939), have indicated that the tetragonal PbO_2 may be reduced to $PbO_{1.66}$ without the appearance of a lattice different from that of PbO_2. Furthermore, they point out, the next lattice encountered in the reduction is that of PbO, which may be either orthorhombic or tetragonal. This would seem to indicate that the lattices of the intermediate oxides do not exist, or that they are merely distortions of the PbO_2 and PbO lattices. And yet, if it were possible to start with PbO_2 and reduce it successively through the various intermediate stages to PbO, a triclinic and a monoclinic system of symmetry would be encountered before reaching the end member, PbO. The following list will illustrate the point.

PbO_2	Tetragonal
$PbO_{1.60}$, (Pb_5O_8)	Tetragonal
$PbO_{1.50}$, (Pb_2O_3)	Triclinic
$PbO_{1.33}$, (Pb_3O_4)	Monoclinic
PbO	Dimorphous

[3] This method consists of placing the focusing lens in front of the telescope and then moving the telescope ocular so that the crystal is somewhat out of focus. If the reflecting surfaces are small enough, a pinhole image of the slit will appear in the spot of light reflected from the surface. Upon rotation of the crystal this image moves in and out of the spot of light just as the signal image in the orthodox arrangement moves in and out of the telescope field. The telescope cross-hairs do not, in this case, offer a reference point for the measurements, but consistent results may be obtained by centering the image in the spot of light. Reference to Table 1 will show that the maximum deviation in using this "pinhole" method on the PbO_2 crystals was 4′.

Pb_5O_8

Pb_5O_8 crystals were first identified by Clark *et al.*,[4] who reported them as having a density of 9.514 and as showing tetragonal symmetry with an axial ratio very nearly equal to 1. Their crystals were too small,—judging from their photomicrograph,—to allow goniometric measurements. Those obtained in this laboratory are evidently considerably larger, some of them being more than one mm. on a side. Although the choice of an axial ratio for Pb_5O_8 based on goniometric measurement alone is rather arbitrary, preliminary investigation of the x-ray powder pattern appearing in Fig. 6 indicates the value given in Table 1.

The crystals of this oxide are jet black, very good reflectors of light, exhibit various interference colors, particularly orange, yellow, and blue, and are often iridescent. This is due to striations caused by a highly characteristic twinning of the crystals parallel to the first order prism face. This parallel growth is also responsible for the 90° re-entrant angles which may be seen in Fig. 2. First order pyramids and basal pinacoids account for nearly all of the area on these crystals, but fragments of both the first and second order prisms may frequently be found. These forms are drawn approximately in their relative sizes in Fig. 3.

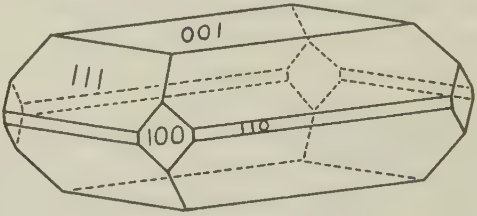

FIG. 3. Typical crystal of Pb_5O_8.

Generally speaking, four types of Pb_5O_8 crystals appear. Large crystals showing only parallel growth are most numerous; such is the one in the lower left-hand corner of Fig. 2. Double crystals like that in the upper right-hand corner of the same figure, and triplets such as that shown in the center are fairly abundant. The aggregates similar to that in the upper left-hand corner of the photomicrograph are less numerous.

Especially interesting is the twinning of the Pb_5O_8 crystals. It occurs on the (101) plane and frequently repeats to form triplets. When either a double or a triple crystal of this oxide forms, it usually grows in such a manner that the faces which are common become considerably larger than any of the others. Thus this common (111) face becomes the natural base of the composite crystal. When the triplet is set upon this base and viewed from above, the normals to the other faces apparently lie so that their projections on the base plane are 60° apart. In other words, the triplet mimics hexagonal symmetry; it appears as though the common face, $(\bar{1}\bar{1}1)$ in the drawing, were a (0001) plane and the others were of the form $\{10\bar{1}1\}$. The twinned nature of the crystal is, however, quite obvious from the re-entrant angles caused by the failure of the various faces of the form $\{111\}$ to coincide. Figure 4 is a stereographic projection of such a triplet.

---

[4] Clark, G. L., *et al.*, *loc. cit.*

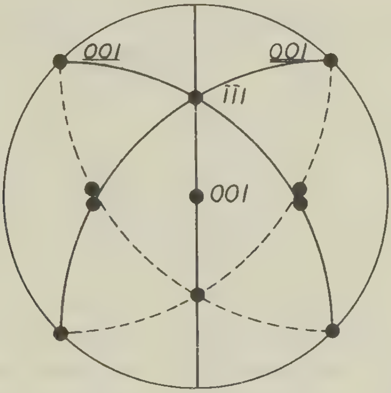

FIG. 4. Stereographic projection of a triplet of Pb_5O_8. Twin-plane = (101). One zone of each of the three crystals is shown. Each zone contains the following faces: (001), $(\bar{1}\bar{1}1)$, $(\bar{1}\bar{1}\bar{1})$, $(00\bar{1})$, $(11\bar{1})$, (111); and the face common to the three crystals is $(\bar{1}\bar{1}1)$.

PbO_2

Lead peroxide is found in various parts of the United States and of Europe as a mineral named plattnerite. It is secondary and usually occurs in nodular or botryoidal masses. Specific gravity determinations give values ranging from 8.5 to 9.45, the lower values being due to porosity and to various impurities, especially limonite. The mineral is coal-black and shows no signs of cleavage or twinning.[5]

Plattnerite was first described as rhombohedral, but the crystals so described were apparently pseudomorphous after pyromorphite.[6] Later investigation by A. F. Ayres showed the mineral to be tetragonal with an axial ratio of 0.67643.[7] But since Ayres' measurements were made on minute crystals, and since he did not indicate the probable error of his measurements, no particular significance can be given to the discrepancy between the ratio indicated by Ayres and that given in Table 1.

---

[5] Dana, E. S., *System of Mineralogy*, Wiley, New York (1920), p. 239.

[6] Greg and Lettsom, *Mineralogy of Scotland* **(1858)**, p. 389.

[7] Yeates and Ayres, *Am. Jour. Sci.*, **43,** 407 (1892).

TABLE 1. ONE-CIRCLE MEASUREMENTS OF PbO_2 AND Pb_5O_8 CRYSTALS

	Angle	No. of meas.	Arith. mean	Max. devia.	Axial ratio
PbO_2	$101\wedge\bar{1}01$	24	68° 19′	4′	0.6785
Pb_5O_8	$111\wedge\bar{1}\bar{1}1$	24	54 26	5	0.989

TABLE 2. TWO-CIRCLE MEASUREMENTS OF PbO_2 CRYSTALS

Form	No. of faces	No. of meas.	Measured (arith. mean)		Computed	
			ϕ	ρ		
101	4	24	90° 00′	34° 9.5′	90° 00′	34° 9.5′
111	4	2	44 30	43 30	45	43 49
211	8	20	63 30	56 30	63 26	56 38
230	8	20	32 32	85	33 40	90

Lead peroxide is also well known as a brown powder[8] used for various industrial and laboratory purposes, but it has never been described in the artificially crystalline state. Indeed, it is evident that lead peroxide has not been recognized as an artificial crystal prior to this study.

M. L. Michel,[9] in 1890, reported having obtained lead peroxide crystals by fusing lead oxide with a certain quantity of potash. In describing the crystals so obtained he relates,

> Ces cristaux sont très brillants, d'un brun foncé; ils affectent la forme de prismes très allongés, suivant l'axe principal; on observe sur la base des lignes de clivage croisées à angle droit; . . .

This description applies to the crystals exhibited in Fig. 1 in so far as the prismatic habit goes, but the crystals presently to be described are jet black, and show no signs of cleavage. As was mentioned above, the natural mineral, plattnerite, is also black, and in contradistinction to Michel's crystals shows no traces of cleavage.

A. Simon[10] reported obtaining lead peroxide crystals in 1930, but it is now apparent that the crystals he pictured in Fig. 1 of his article and designated as PbO_2 were not tetragonal PbO_2, but triclinic Pb_2O_3.

---

[8] *X*-ray diffraction patterns of this powder give the PbO_2 lattice as tetragonal, body centered, with $a=4.96$ to 4.98, $c=3.39$ to 3.40. (*Str. Ber.*, **1**, p. 211; and *Int. Crit. Tab.*, **1**, p. 342.)

[9] Michel, M. L., *Bull. Soc. Min.*, **13**, 56 (1890).

[10] Simon, A., *Zeits. anorg, allgem. Chem.*, **185**, 300 (1930).

On the PbO_2 crystals recently obtained two crystallographic forms are preponderant. Second order pyramids account for most of the area at the ends, while the lateral area is made up by the ditetragonal prism {230}. Other forms which occur,—{111} and {211},—are usually so small as to give mere points of reflected light. Figure 5 is a clinographic projection of the twinned PbO_2 showing the forms {101}, {211}, and {230}. The (211) faces are relatively larger in the drawing than on the actual crystals. Of the forms mentioned by Ayres as appearing on plattnerite, only the {101} appears on the artificial crystals measured.

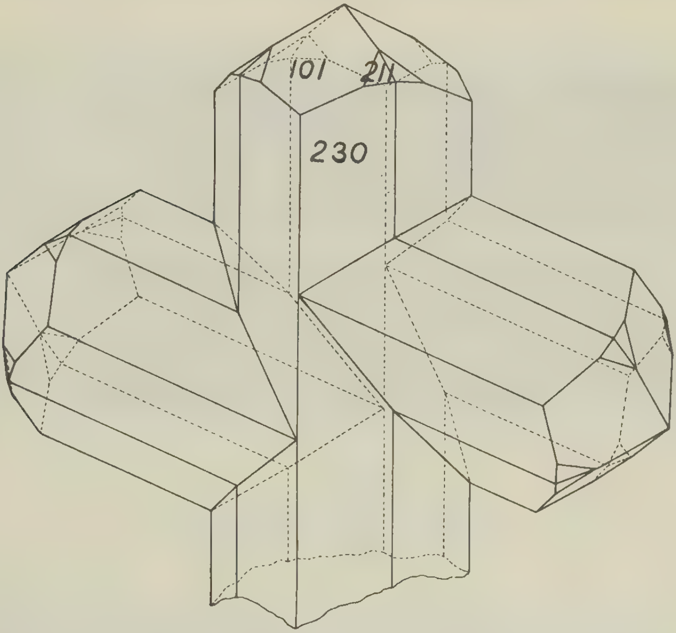

FIG. 5. Twin-crystal of PbO_2; twin-plane = (101).

Figure 1 shows that the prism faces of the PbO_2 taper toward the extremities of the crystals. Although this taper is fairly constant at 85° on the crystals measured, it has no simple index and must therefore be ascribed to oscillatory growth. The measured angle of the prism also diverges from the computed angle, but this is due to the difficulties of measurement. No signal was obtainable from the face, and it was too large to give a pinhole image.

In common with many other tetragonal minerals, PbO_2 twins on the plane (101), (see Fig. 5); and this particular habit of growth,—not described in plattnerite,—is the only one observed on the many crystals examined. Nearly all are crosses of the type shown in Fig. 1. Some few specimens such as the one shown in the upper right-hand part of that figure, and a fair number of interlaced crosses in clusters were found. But the great mass of the crystals are simple, slender needles crossing at an angle of 68°. In size they range from microscopic dimensions up to nearly 3 mm.

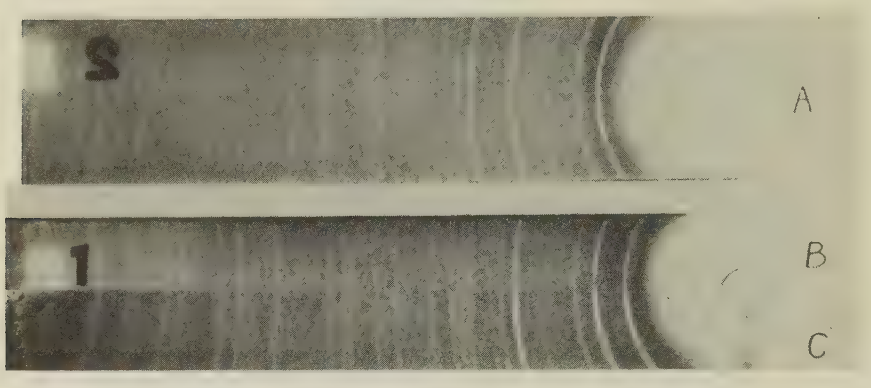

Fig. 6.
A....Pb_5O_8
B....PbO_2 crystals
C....PbO_2 c.p. powder

In Fig. 6 will be found three *x*-ray powder patterns. One is of the Pb_5O_8 crystals; the other two are of PbO_2 crystals and c. p. powder. Those lines which appear on the c. p. lead peroxide pattern but not on that of the crystals of PbO_2 are due to impurities,—especially lead monoxide,—in the powder.

The author wishes to express his gratitude for the indispensable help of Professor Max Petersen of Lehigh University, who prepared the crystals described and made possible this study. He also wishes to thank Dr. R. D. Butler of this university and Dr. Clifford Frondel of the Harvard University Mineralogical Museum for their gracious advice and criticism. Dr. Samuel G. Gordon of the Academy of Natural Sciences, Philadelphia, provided a specimen of plattnerite for comparative observations in connection with the study of PbO_2, and for this generous gift the author records his obligation.

UNIT CELL AND SPACE GROUP OF VRBAITE ($Tl(As,Sb)_3S_5$), SELIGMANNITE ($CuPbAsS_3$) AND SAMSONITE ($Ag_4MnSb_2S_6$)

CLIFFORD FRONDEL,
*Harvard University, Cambridge, Massachusetts.**

ABSTRACT

The following data were obtained by the Weissenberg equi-inclination method. Vrbaite from Allchar: space group *Cmca;* $a_0=13.35$, $b_0=23.32$, $c_0=11.23$ (all ± 0.05); $a_0:b_0:c_0=0.5725:1:0.5815$; cell contents $Tl_{21}(As,Sb)_{63}S_{105}$. Samsonite from Andreasberg: space group $P2_1/n$; $a_0=10.29$, $b_0=8.05$, $c_0=6.61$ (all ±0.05), $\beta=92°41'$ (morph.); $a_0:b_0:c_0=1.278:1:0.821$; cell contents $Ag_8Mn_2Sb_4S_{12}$. Seligmannite from Bingham: space group *Pnmm;* $a_0=8.04$, $b_0=8.66$, $c_0=7.56$ (all ±0.05); $a_0:b_0:c_0=0.928:1:0.873$; cell contents $Cu_4Pb_4As_4S_{12}$.

X-ray powder photographs of aikinite, $CuPbBiS_3$, indicate that it is not a member of the seligmannite-bournonite group.

VRBAITE ($Tl(As,Sb)_3S_5$)

Vrbaite, one of the few known thallium minerals, has been found only at Allchar, northwest of Salonika, Greece. The morphological description of Ježek (1912) established the point symmetry as $2/m\ 2/m\ 2/m$—orthorhombic dipyramidal. The single chemical analysis available, by Křehlík (1912), affords the formula $Tl(As_{.68},Sb_{.32})_3S_5$. The close approach of the As:Sb ratio to 2:1 is here taken as fortuitous. The artificial compound $TlAs_3S_5$ has been found in the system Tl_2S-As_2S_3 by Canneri and Fernandes (1925), but the identity of this substance with vrbaite has not been shown.

A natural crystal from Allchar[1] was examined by the Weissenberg equi-inclination method, using Cu radiation. The interpretation of the films followed the plane group method of Buerger (1935). Rotation photographs were taken about the principal axes, together with 0-, 1- and 2-layer photographs about [100], 0- and 1-layers about [010] and a 0-layer about [001]. The position and intensity of the diffraction effects was entirely consistent with orthorhombic centrosymmetry. The stacking sequence of the reciprocal lattice levels in the {100} projections involved a translation of the 1-layer of $c/2$ and established the lattice type as C-centered. Systematic omissions in the 0-layer about [010] defined a glide {010} in the direction [001], and an additional glide {001} in the direction [100] was defined by the 0-layer about [001]. The space group is $D_{2h}^{18}=Cmca$, in accordance with the holohedral morphology. The orientation of the structural cell $(c<a<b)$ conforms with the choice of morphological cell by Ježek. The cell dimensions calculated from high order reflections on the 0-layers are given below, together with the x-ray and morphological ratios.

---

* *Contribution from the Department of Mineralogy and Petrography, Harvard University, No. 233.*

[1] From the Roebling collection of the United States National Museum. No.: R939. Loaned through the courtesy of Dr. William F. Foshag, Curator.

$a_0=13.35$ $b_0=23.32$ $c_0=11.23$ (all ±0.05)
$a_0:b_0:c_0=0.5725:1:0.4815$
$a:b:c=0.5659:1:0.4836$ (Ježek)

The number of formula units in the unit cell, taking the molecular weight as 534.5 and the specific gravity[2] as 5.3, is 21.0. The calculated specific gravity for Z=21 is 5.29.

SELIGMANNITE ($CuPbAsS_3$)

Seligmannite is the arsenical analogue of bournonite, $CuPbSbS_3$. Morphological study of material from the Binnenthal by Baumhauer (1901, 1902) and by Solly (1903, 1905, 1912) established the point symmetry as $2/m\ 2/m\ 2/m$—orthorhombic dipyramidal. Chemical analyses later contributed by Prior (1908) yielded the formula given above and confirmed the close relation to bournonite indicated by the morphology. The crystallography of the only other known occurrence of the mineral, at Bingham, Utah, was described in 1928 by Palache. A quantitative analysis of this material was not given, but blowpipe and microchemical tests proved the absence of Sb and the presence of As.

A Weissenberg study was made of one of the original crystals from the Bingham occurrence. Cu radiation was used. The crystal was rather large and poorly shaped for x-ray work, and contained a very small irregular portion of another crystal from which it had been broken. Rotation photographs were taken about the principal axes, together with 0-layers about [100] and [001] and a 0- and 1-layer about [010]. The reciprocal lattice was plotted for all of the films to make certain the identification of adventitious spots due to the inclusion mentioned. Nothing was found in the position or intensity of the spots clearly proper to the main body of the crystal that required other than orthorhombic centrosymmetry. The projections on {010} established the lattice type as primitive, and the {100} projection defined a diagonal glide {100} with component $b/2+c/2$. Other special diffraction effects were absent. The space group is thus either $C_{2v}{}^7=Pnm$ or $D_{2h}{}^{13}=Pnmm$. The morphology indicates holohedral symmetry so that the correct space group is $Pnmm$.

---

[2] Ježek gives three observed values for the specific gravity· 5.271 on 0.272 g. with the pycnometer, 5.333 on 0.272 g. by a hydrostatic method, and 5.302 on 0.458 g. with the pycnometer.

The cell dimensions calculated from high order reflections on the 0-layers are given in Table 1, beyond. The cell contents are 4($CuPbAsS_3$). The observed specific gravity, obtained by the writer on a single small crystal on the microbalance, is 5.38, and the calculated specific gravity is 5.54. The seligmannite from the Binnenthal has G. = 5.44, 5.48, and As:Sb $\sim$ 41:1. Bournonite has an observed specific gravity of 5.83 ± 0.03, and a calculated value of 5.93 (from the cell dimensions of Oftedal (1932) cited in Table 1).

The *x*-ray data confirms the isostructural relation of seligmannite and bournonite indicated by the morphology and chemistry, as summarized in Table 1. A complete isomorphous series between these species may exist in point of As-Sb content, but the available analyses show an apparent maximum substitution of As for Sb at about Sb:As = 4:1 at the bournonite end of the series. The composition of these minerals suggests that their structural scheme is of a distorted sphalerite- or wurtzite-type. The pseudocubic cell may be remarked in this connection.

TABLE 1. COMPARISON OF SELIGMANNITE AND BOURNONITE

	Cell Contents	*X*-ray Cell			Morphological Cell			Space Group
		a_0	b_0	c_0	a	b	c	
Seligmannite	$Cu_4Pb_4As_4S_{12}$	8.04	8.66	7.56	0.9233	1	0.8734	*Pnmm*
					(Binnenthal)			
		0.928	1	0.873	0.9217	1	0.8718	
					(Bingham)			
Bournonite	$Cu_4Pb_4Sb_4S_{12}$	8.10	8.65	7.75	0.9380	1	0.8969	*Pnmm*
					(Brooke and Miller (1852))			
		0.936	1	0.896				

Aikinite, $CuPbBiS_3$, has been classed with bournonite and seligmannite on the basis of the similarity in composition. Adequate crystallographic data are lacking. *X*-ray powder photographs of aikinite from Berezov differ markedly from those of seligmannite and bournonite, and the mineral probably does not belong in this group.

SAMSONITE ($Ag_4MnSb_2S_6$)

Samsonite is known only from the Samson vein, Andreasberg, in the Harz, Germany. The only analysis available, cited in the original description of Werner and Fraatz (1910), is in very close agreement with the formula given above. The existing morphological data for the species is summarized in a recent study by Palache (1934). The point symmetry is 2/*m*—monoclinic prismatic.

A Weissenberg study was made of a measured crystal, employing Cu radiation. Rotation and 0-layer photographs were taken about the principal axes and a 1-layer about [010]. The position and intensity of the diffraction effects were in accordance with monoclinic centrosymmetry. The lattice type, established by the stacking plan of the 0- and 1-layers about [010], is primitive. A diagonal glide {010} with component $a/2+c/2$ was defined by the 0-layer about [010], and a two-fold screw axis was defined along [010]. The space group is $C_{2h}^5=P2/_1n$, confirming the holohedral morphology. The cell dimensions as calculated from high order reflections on the 0-layers are cited below, together with the morphological ratio as averaged by Palache (1934) from the closely agreeing measurements of four observers. The x-ray value for β, calculated from [301]*, a^* and c^*, is less accurate than the morphological value.

$$a_0=10.29 \qquad b_0=8.05 \qquad c_0=6.61 \qquad \text{(all } \pm 0.05)$$
$$a_0:b_0:c_0=1.278:1:0.821 \quad \beta=92°2'$$
$$a:b:c=1.2782:1:0.8198 \quad \beta=92°41'$$

The specific gravity of samsonite was determined on the microbalance by the writer as 5.51. The number of formula units associated with the cell, taking $\beta=92°41'$, are then $1.98\sim 2$, or $Ag_8Mn_2Sb_4S_{12}$ for the cell contents. The calculated specific gravity for $Z=2$ is 5.56. The monoclinic modification of Ag_3SbS_3 (pyrostilpnite) has an observed specific gravity of 5.94.

References

Baumhauer, H., *Akad. Wiss. Berlin, Sitzber.*, 110 **(1901).**

Brooke, H. J., and Miller, W. H., *Introduction to Mineralogy*, London, 201 **(1852).**

Buerger, M. J., *Zeits. Kryst.*, **91,** 255 (1935).

Canneri, C., and Fernandes, F., *Atti Accad. Lincei, Roma*, **1,** 671 (1925).

Ježek, B., *Zeits. Kryst.*, **51,** 365 (1912).

Křehlík, F., *Zeits. Kryst.*, **51,** 379 (1912).

Oftedal, I., *Zeits. Kryst.*, **83,** 157 (1932).

Palache, C., *Am. Mineral.*, **13,** 402 (1928).

Palache, C., *Am. Mineral.*, **19,** 194 (1934).

Prior, G. T., *Min. Mag.*, **15,** 385 (1910).

Solly, R. H., *Min. Mag.*, **13,** 336 (1903).

Solly, R. H., *Min. Mag.*, **14,** 186 (1906).

Solly, R. H., *Min. Mag.*, **16,** 282 (1912).

Werner and Fraatz, *Cbl. Min.*, 331 **(1910).**

THE RELATION BETWEEN COLOUR AND CHEMICAL COMPOSITION IN THE BIOTITES

A. Jean Hall, *University of Cape Town, South Africa.*

Abstract

The results of plotting the analyses of many biotites indicate that the colours of the more common biotites are dependent upon their relative contents of iron, magnesia and titania. Iron is responsible for producing the green colours of biotites, while titania gives the brown and red colours. Magnesia appears to be able to dilute or mask the colour effect produced by titania.

During a study of metamorphic biotites the author was led to certain conclusions as to the relation between the colour and the chemical composition of the biotites. In order to confirm these conclusions, the analyses of as many similar biotites as possible were collected from the literature of the past thirty years and plotted together with the biotites analyzed by the author.

The biotites chosen for this study all contain FeO in excess of Fe_2O_3, while their MnO content is not in excess of 0.50%. In most cases the Cr_2O_3 content has not been reported, but where it is given, as in the case of some of Grout's biotites, it is very small. The oxides used for plotting on the triangular diagram in Fig. 1 are TiO_2, total FeO (Fe_2O_3+FeO all expressed as FeO) and MgO. The percentage values of these oxides will be found in Table 1, together with the pleochroic colour of γ, and the name of the author whose analysis has been used. Several more biotite analyses might have been taken from recent literature were it not for the unfortunate fact that so many authors neglect to state the pleochroic colours with their analyses. Sixteen analyses were carried out on material collected by the author, which, it is hoped, will be published fully later.

According to Heddle's (18) definition of biotite, haughtonite and lepidomelane, the proportion of FeO:Fe_2O_3 in haughtonite is 4:1, in biotite 25:1 and in lepidomelane 1:9. The majority of the micas given in Table 1 vary between haughtonite and true biotite, while those containing large amounts of MgO and low FeO grade towards phlogopites, and those with little or no MgO are siderophyllites.

From the consideration of the triangular plot of the oxides given in Fig. 1 the author was led to the conclusion that the red-brown colour of many of the biotites was due to their high titania content. Some of the brown biotites, however, contain as much or more titania than some of the red-brown ones, but also contain more magnesia. It is therefore suggested that the magnesia has the effect of diluting or masking the colour produced by the titania. In a spectroscopic study of the colour of tourmaline, Warner (19) has found that magnesia has no influence upon the colours produced by iron and manganese in this mineral, but it would appear that in the biotites a high magnesia content has the effect of masking the colour due to titania.

The blue-green biotites described by some authors (see Table 1) owe their colour solely to their iron content, since they have little or no titania. Greenish-brown biotites, on the other hand, may be produced in two different ways. In the case of Woodland's biotite from Hendre, there is a high iron content accompanied by some titania and low magnesia. Greenish-brown biotites at the other end of the field have a low iron content with sometimes an appreciable amount of titania masked by high magnesia. The intensity of colour of these latter biotites is much less than that of the former.

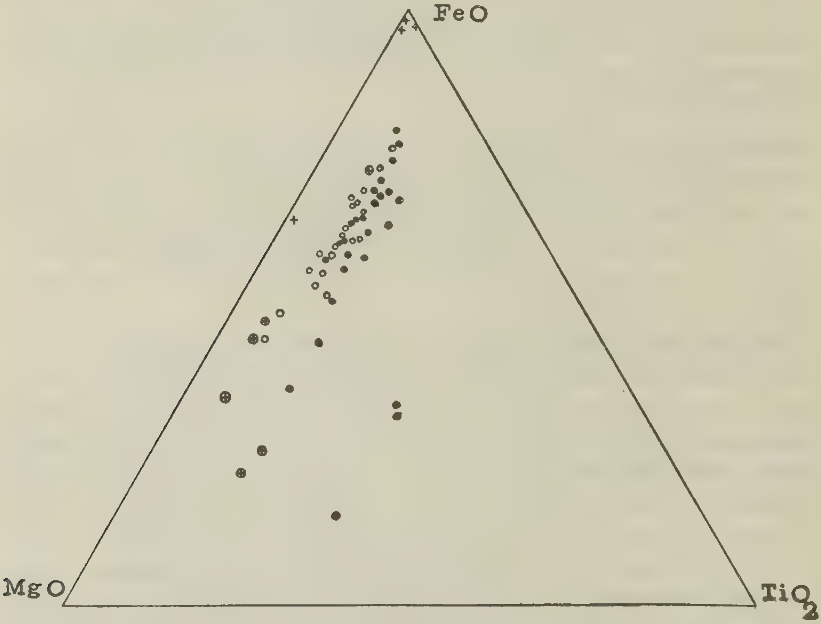

FIG. 1. Triangular plot of total FeO-TiO_2-MgO for the biotites.
+ = green or blue green. ⊕ = brownish green.
○ = brown. ● = red brown or red.

Freudenberg's wodanites and Prider's titano-phlogopite will be seen to occupy positions towards the centre of the diagram in Fig. 1, which they hold by reason of their high content of titania. Beyond a certain amount of titania, the red or red-brown colour will still be maintained even though the magnesia is high.

TABLE 1

No.	Author	Fe_2O_3	FeO	Total FeO	TiO_2	MgO	Colour of γ
1	Nockolds[1]	0.79	20.98	21.69	0.21	0.46	blue-green
2	Harada[2]	1.55	25.50	26.90	—	0.54	green
3	Kranck[3]	9.12	21.62	29.83	tr	0.72	blue-green
4	Phillips[4]	7.37	11.25	17.88	0.23	9.84	blue-green
5	Phillips[4]	1.73	13.23	14.79	1.72	14.93	greenish brown
6	Grout[5]	7.44	7.72	14.42	1.67	16.55	green
7	Brauns[6]	2.02	6.77	8.59	5.14	19.61	greenish brown
8	Kranck[7]	1.46	6.02	7.33	4.90	20.88	greenish brown
9	Hall*	3.33	6.73	9.73	1.66	17.00	brownish green
10	Woodland[8]†	7.24	21.04	27.54	2.85	7.44	brownish green
11	Grout[5]	1.14	23.75	24.78	2.73	6.16	brown
12	Grout[5]	3.03	23.23	25.96	3.32	9.24	brown
13	Grout[5]	4.05	14.80	18.44	2.23	10.21	brown
14	Hess[9]	2.26	14.81	16.84	2.64	8.45	deep brown
15	Seidel[10]	4.88	16.92	21.41	2.63	7.91	brown
16	Seidel[10]	3.96	10.12	13.68	1.95	15.21	brown-yellow
17	Tsuboi[11]	4.49	15.00	19.04	3.29	11.80	dark sepia brown
18	Tsuboi[11]	3.37	20.15	23.18	2.77	7.20	dark brown
19	Tsuboi[12]	2.95	18.87	21.53	3.07	9.52	Vandyke brown
20	Tsuboi[12]	3.00	18.83	21.53	3.15	9.61	Vandyke brown
21	Tsuboi[12]	1.86	26.17	27.84	3.64	5.16	Vandyke brown
22	Seidel[10]	3.03	12.45	15.18	1.86	13.78	yellow brown
23	Deer[13]	3.22	19.94	22.84	3.48	8.23	yellow brown
24	Deer[13]	2.48	19.07	21.30	3.63	11.62	yellow brown
25	Hall*	2.79	14.26	16.77	3.90	11.28	brown
26	Hall	2.59	14.40	16.73	2.95	11.42	brown
27	Hall*	2.79	14.84	17.34	2.20	11.13	brown
28	Hall	2.73	17.08	19.54	3.74	8.70	brown
29	Hall	3.46	16.92	20.04	4.21	8.52	brown with reddish tinge
30	Hall	1.62	16.02	17.48	4.59	12.05	reddish brown
31	Tsuboi[11]	1.00	20.09	21.99	2.52	8.03	brown with reddish tinge
32	Tsuboi[14]	2.10	26.80	28.69	3.33	4.98	mars brown
33	Tsuboi[12]	.77	21.42	22.11	3.28	6.40	madder brown
34	Tsuboi[12]	.69	18.11	18.73	2.99	8.80	etruscan red
35	Tsuboi[12]	.76	18.39	21.48	4.86	11.90	English red
36	Tsuboi[12]	.87	21.10	21.88	3.29	8.71	madder brown
37	Tsuboi[12]	.87	20.88	21.66	3.53	8.08	orange rufous
38	Tsuboi[12]	.27	19.46	19.70	4.07	7.86	burnt orange
39	Tsuboi[12]	.68	16.88	17.49	2.65	9.78	orange rufous
40	Tsuboi[12]	1.05	26.34	27.28	3.79	5.51	madder brown
41	Seidel[10]	4.70	17.09	21.32	3.22	10.00	red brown
42	Chapman[15]	nil	15.52	15.52	5.22	14.23	deep red brown
43	Chapman[15]	8.00	23.54	30.74	2.94	4.97	chestnut brown
44	Deer[13]	2.90	18.30	20.91	3.99	10.42	reddish brown
45	Hall	1.42	19.27	20.55	4.99	9.78	red brown
46	Hall*	1.03	20.56	21.49	3.05	8.62	pale red brown
47	Hall	2.60	19.17	21.51	3.68	6.00	red brown
48	Hall	1.83	21.54	23.19	3.52	6.20	red brown
49	Hall	2.39	20.99	23.14	4.31	6.14	red brown
50	Hall*	3.16	20.34	23.18	4.01	7.34	red brown
51	Hall	1.51	20.53	21.89	5.27	7.28	red brown
52	Hall*	3.05	22.06	24.81	5.40	6.59	red brown
53	Nockolds	1.53	10.97	12.35	5.08	16.87	red brown
54	Freudenberg[16]	1.01	11.09	12.00	12.02	13.11	red brown
55	Freudenberg[16]	3.09	10.63	13.41	12.56	13.80	red brown
56	Prider[17]	2.18	3.73	5.69	12.02	19.66	reddish brown

* Analyst: N. Sahlbom.

† Analyst: A. J. Hall.

It is hardly to be expected that the colour of such a complex system as the biotites could be easily explained by such a simple theory as that given above, but it will be seen from Fig. 1 that the results are sufficiently good to justify the assumption that the theory is fairly correct. In considering the relation of chemical composition to colour in the biotites, it is not the absolute amount of any oxide present which produces the colour effect, but the proportion of that oxide to those of the others present. Thus, red-brown biotites are generally high in titania and iron and low in magnesia, but, if the proportion of titania is sufficiently high, the biotite will still be red-brown even though the magnesia is high and the iron low.

We may draw the further conclusion from the diagram (Fig. 1) that colour is very little real indication of the composition of a biotite. This will become evident if we tabulate the results of Fig. 1 as follows:—

$$\text{Red-brown biotite}=\begin{cases}\text{High } TiO_2+\text{high } FeO+\text{low } MgO\\ \text{High } TiO_2+\text{low } FeO+\text{high } MgO\end{cases}$$

$$\text{Blue-green biotite}=\begin{cases}\text{High } FeO-TiO_2+\text{low } MgO\\ MgO\neq FeO-TiO_2\end{cases}$$

$$\text{Greenish-brown biotite}=\begin{cases}\text{High } FeO+\text{low } TiO_2+\text{low } MgO\\ \text{Low } FeO+TiO_2+\text{high } MgO\end{cases}$$

$$\text{Brown biotite}=\begin{cases}\text{High } FeO+\text{low } TiO_2+\text{low } MgO\\ FeO=MgO+\text{low } TiO_2\end{cases}$$

It will be seen that each of the various colour varieties of biotite may be formed in two different ways. It will also appear from the above that the colour effect produced by titania is dominant over that produced by iron unless titania is masked by a large amount of magnesia.

It is rather difficult to discover whether iron present as Fe_2O_3 has any influence on the colour of biotite as distinct from that present as FeO, since no analyses are reported containing Fe_2O_3 only without much FeO or TiO_2. It will be observed, however, that Kranck's siderophyllite contains 9.12% Fe_2O_3 and is still bluish-green. The micas described by Jakob (20) and Magnusson (21) from Långban appear to owe their red-brown colour to their manganese content, since they are high in MnO and low in FeO and TiO_2. These are somewhat exceptional micas, and in general it may be said that biotite does not contain sufficient manganese for this element to have any effect upon the colour, and no doubt the same is also true of chromium.

ACKNOWLEDGMENT

The work contained in this paper was carried out in the Department of Mineralogy and Petrology, Cambridge, England. The author wishes to thank Professor C. E. Tilley for helpful discussion and advice during the course of the work, Dr. S. R. Nockolds for permitting the use of one of his unpublished biotite analyses (biotite No. 53 in Table 1) and Dr. A. W. Woodland of the Geological Survey of Great Britain for supplying material for the biotite analysis No. 10. A grant from the Royal Society, London, to defray the cost of six of the biotite analyses of the author's material is also gratefully acknowledged.

REFERENCES

(1) NOCKOLDS, S. R., and RICHEY, S. E., Replacement veins in the Mourne Mountains granites, N. Ireland: *Am. Jour. Sci.*, **237**, 38 (1939).

(2) HARADA, Z., Chemische Analysenresultate von japanischen Mineralien: *Jour. Fac. Sci. Imp. Un. Hokkaido*, **3**, ser. 4, 319 (1936).

(3) KRANCK, E. H., A beryl-bearing pegmatite from Uuku in Carelia: *Bull. Com. Géol. Finlande*, No. **85**, 70–77 (1929).

(4) PHILLIPS, F. C., Some mineralogical and chemical changes induced by progressive metamorphism in the Green Bed group of the Scottish Dalradian: *Min. Mag.*, **22**, 239–255 (1930).

(5) GROUT, F. F., Notes on biotite: *Am. Mineral.*, **9**, 159 (1924).

(6) BRAUNS, R., Die chemische Zusammensetzung von Augit und Biotit je aus tephritischer Lava und aus Lacher Trachyt: *N. Jahrb. Min., B.*, **57A**, 131 (1928).

(7) KRANCK, E. H., On turjaite and the ijolite stem of Turga, Kola: *Fennia*, **51**, 104 (1928).

(8) WOODLAND, A. W., Petrological studies in the Harlech Grit: *Geol. Mag.*, **75**, 369 (1938).

(9) HESS, F. L., Cæsium biotite from Custer County, South Dakota: *Am. Mineral.*, **17**, 173–176 (1932).

(10) SEIDEL, P., Diss. Univ. Zurich, 1906: *Zeits. Krist.*, **57**, 416 (1923).

(11). TSUBOI, S., Petrological notes: *Jap. Jour. Geol., Geogr.*, **12**,, 112 (1935).

(12) TSUBOI, S., Petrological notes: *Jap. Jour. Geol., Geogr.*, **15**,, 125–129 (1938).

(13) DEER, W. A., The composition and paragenesis of the biotites of the Carsphairn igneous complex: *Min. Mag.*, **24**, No. 156, 495–502 (1937).

(14) TSUBOI, S., Petrological notes: *Jap. Jour. Geol., Geogr.*, **13**, 335 (1936).

(15) CHAPMAN, R. W., and WILLIAMS, C. R., Evolution of the White Mountain magma series: *Am. Mineral.*, **20**, 502–530 (1935).

(16) FREUDENBERG, W., Titanobiotit vom Katzenbuckel: *Mitt. Bad. Geol. Landesanst. Heidelberg*, **8**, 317–340 (1919).

(17) PRIDER, R. T., Some minerals from the leucite-rich rocks of the West Kimberley area, Western Australia: *Min. Mag.*, **25**, No. 166, 373–387 (1939).

(18) HEDDLE, F. (Ref. P. Groth), *Zeits. Krist.*, **5**, 620 (1881).

(19) WARNER, T. W., Spectrographic analysis of tourmaline with correlation of colour and composition: *Am. Mineral.*, **20**, 531 (1935).

(20) JAKOB, J., Beiträge zur chemischen Konstitution der Glimmer. I. Mitt. Die schwedischen Manganophylle: *Zeits. Krist.*, **61**, 153–163 (1924).

(21) MAGNUSSON, N. H., Långbans Malmtrakt: *Sver. Geol., Under Beskrivning. Ser. ca. No.* **23**, 1930.

THE RELATION BETWEEN CHEMICAL COMPOSITION AND REFRACTIVE INDEX IN THE BIOTITES

A. Jean Hall, *University of Cape Town, South Africa.*

Abstract

It is suggested that the relation between the chemical composition and the refractive index of the biotites should be considered from the point of view of the substitution of the metal atoms in the structural formula. The influence of Fe'', Fe''', Ti'''' and probably also Ti''', Mn'', Zr'''', Cr''', etc., upon the refractive index must be taken into account. This is illustrated by plotting the values of total iron against γ for a large number of biotites analyzed during recent years.

The present work is the outcome of an investigation of the biotite system to ascertain how far the refractive index of a biotite is an indication of its chemical composition. As a result of this investigation it is believed that previous workers on this subject have over-simplified the matter and that the relationship is a much more complicated one than has been supposed. In A. N. Winchell's (1) studies on the biotite system, the various biotites are calculated into molecules for the purpose of plotting their composition against their refractive indices. In these molecules Winchell omits lime, calculates ferric iron as ferrous, MnO and TiO_2 as FeO, F as OH, and Na_2O as equivalent to K_2O. After a study of the reliable analyses of biotite reported during recent years, the author believes that these complex minerals cannot be treated in such a simple manner but that the influence on the refractive index of several of the oxides present in the biotite must be taken into account.

It is suggested that the biotites should not be studied as molecules in relation to their refractive indices, but that we should consider them from the point of view of the substitution of the various atoms in the structural formula. We may first consider which atoms are likely to play a part in influencing the refractive index of the biotites. We may feel fairly certain that Fe'', Fe''' and Ti, when substituted for Mg in increasing amounts, are liable to raise the refractive index. The parts played by Mn, Zr and Cr are more difficult to assess owing to the fact that few biotites contain appreciable amounts of these elements or at least, especially in the case of the two latter, the amounts present are seldom sought after. The author disagrees with Winchell and Jakob in their statements that biotites do not contain lime, since many reliable analysts report small amounts of CaO. However, again in the case of Ca we have very little data from which to draw any conclusions as to its effect, if any, on the refractive index. As regards fluorine, the substitution of the hydroxyl group by this element very probably brings about a lowering of the refractive index, since, if we may argue from analogy, minerals which have a high fluorine content have a low refractive index (cf. fluorite and calcite, sellaite and magnesite).

There is the further probability that elements in a higher state of oxidation exert a greater influence on the refractive index than those at a lower state. Two of Larsen's (2) biotites from the San Juan Region, Colorado, may be compared with two analyzed by Tsuboi (3), as follows.

	Fe_2O_3	FeO	Total FeO	TiO_2	γ
Larsen	17.13	1.85	17.27	3.63	1.720
Larsen	17.71	0.53	16.46	4.19	1.723
Tsuboi	0.27	19.46	19.70	4.07	1.646
Tsuboi	0.76	18.39	21.48	4.68	1.658

Tsuboi's biotites contain approximately the same amount of TiO_2 and have higher total iron than Larsen's, yet their refractive indices are very much lower. Fluorine is not reported in Tsuboi's analyses, but from the summation the amount, if any, present cannot be very great. Kunitz (4) has shown that the oxidation of FeO in biotite raises the refractive index N_g, for example from 1.667 to 1.718 for a change from 6.51% Fe_2O_3 and 17.83% FeO in natural biotite to 24.89% Fe_2O_3 in the same mineral after heating. Kôzu and Yoshiki (5) have found that, on heating a biotite, the value of γ is raised from 1.655 to 1.703. Winchell (1*b*) believes that biotite as found contains some Fe_2O_3, but that those which "contain much Fe_2O_3 do so only as a result of oxidation of FeO in the crystal by natural processes." Whether this statement is correct or not, it is nevertheless a fact that petrologists, when dealing with biotites occurring in rocks, frequently find that they contain an appreciable amount of Fe_2O_3 and therefore the influence of this oxide on the refractive index must also be taken into account.

Titanium present in the form of Ti_2O_3 may have also a different effect upon the refractive index than when it is present as TiO_2. Jakob and Parga-Pondal (6) have found that biotites do contain Ti_2O_3, but, in the absence of sufficient data, the influence of this lower oxide on the refractive index cannot be ascertained at present.

Winchell states that "some variation between the indicated and actual optic properties must be expected" since his diagram makes no attempt to show the effect of the oxides of the various elements mentioned above on the optic properties. It is, however, believed that his method of representing the relation of chemical composition to optic properties in the biotites by means of a square diagram is wrong, since many of the titania-iron biotites have higher refractive indices than those given in the few reported analyses of siderophyllite. To illustrate this statement we may plot the refractive indices of several biotites against their iron content. The results will be seen in Fig. 1. The analyses used for this graph have been taken from the literature published during the last forty years. Some new analyses by the author are also included and also some hitherto unpublished analyses of biotites by Dr. S. R. Nockolds. In order to plot the iron content against refractive index (γ), the amount of Fe_2O_3 present must be neglected for the moment and the total iron plotted as FeO. The values of Fe_2O_3, FeO, total FeO, and TiO_2 for these biotites are given in Table 1, with also, in some cases the values of MnO and ZrO_2. Unless stated to the contrary, the values of MnO, ZrO_2 and Cr_2O_3 are less than 0.50%.

It can be seen from Fig. 1 that the biotites occupy two main fields. Those biotites which contain iron and titania are mainly grouped in field 1, while those containing iron, titania and MnO in excess of 0.50% lie in field 2. The points 12, 14, 15 and 16 are biotites whose analyses are given by von Eckermann, Jakob and Karvano and which contain rather less TiO_2 than most other biotites with the same amount of iron. Thus, the values of the refractive indices of these biotites are less than those of the biotites which occupy field 1. Points 1 and 41 represent biotites described by Nockolds and Chapman which contain more titania than other biotites with the same iron content, so that their refractive indices have higher values than the biotites of field 1. The position in Fig. 1 of Chapman's biotite (No. 42) cannot, however, be accounted for so easily. Grout's biotite No. 9 has a higher refractive index than would be expected from its iron and titania content, but contains 1.65% ZrO_2, which may account for its high refractive index. Prider's titaniferous-phlogopite (No. 59) will be seen to have a refractive index far ahead of other biotites with a higher iron content.

Nockolds' and Kranck's siderophyllites (Points 5 and 17), which contain very little or no titania, have much lower refractive indices than comparable iron-titania biotites in field 1. Nockolds' siderophyllite admittedly contains 2.03% fluorine, which might be expected to lower its refractive index. Fluorine is not reported in Kranck's siderophyllite, but, from the summation of the analysis, there can be very little if any there. On the other hand, Kranck's siderophyllite contains 9.12% Fe_2O_3 to 21.62% FeO which might be expected to raise the refractive index beyond that of a purely ferrous iron siderophyllite. It is very much to be regretted that the other analyses of siderophyllite from Pike's Peak (18) and Tanokamiyama, Japan (19) are not accompanied by statements of their refractive indices. Owing to the scantiness of the data it cannot definitely be established that siderophyllite has a lower refractive index

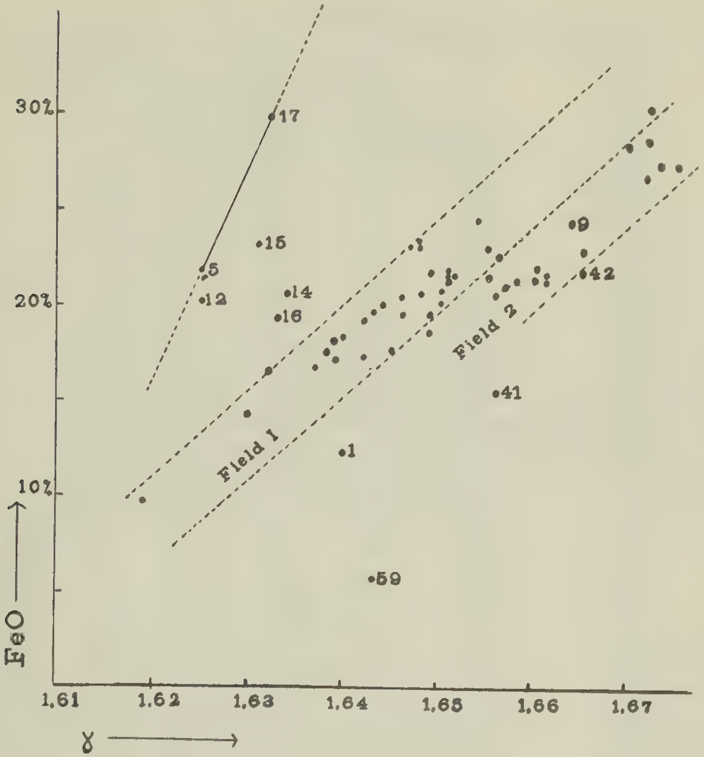

FIG. 1. Plot of total FeO against γ for the biotites. Numbers correspond to the biotites listed in Table 1.

Field 1 contains iron-titanium biotites.

Field 2 contains iron-titanium biotites which in most cases have more than 0.50% MnO.

than the titania-bearing biotites, but it would appear to be highly probable that this is the case.

Kunitz (20) has shown that the refractive index of biotite increases with increasing titania content when the amount of iron remains practically constant. He found that the relationship between increase in titania and increase in refractive index can be expressed by a straight line. From the graph given by Kunitz it appears that the amount by which the refractive index is raised for an increase of 1.0% TiO_2 is .01. This seems to be somewhat excessive as the following calculations will show.

It might be suppposed that if we knew the refractive index of a biotite containing iron, we could calculate from observed values the refractive index of a biotite containing the same amount of iron plus a certain

TABLE 1

No.	Author	γ	Fe_2O_3	FeO	Total FeO	TiO_2	
1	Nockolds	1.640	1.53	10.97	12.35	5.08	
2	Nockolds	1.645	3.41	14.86	17.93	3.54	
3	Nockolds	1.649	4.41	15.84	19.81	3.11	
4	Nockolds	1.655	7.04	16.91	23.25	3.12	
5	Nockolds[7]	1.625	0.79	20.98	21.69	0.21	
6	Grout[8]	1.630	7.44	7.72	14.42	1.67	
7	Grout[8]	1.640	4.05	14.80	18.44	2.23	
8	Grout[8]	1.655	3.03	23.23	25.96	3.32	
9	Grout[8]	1.664	1.14	23.75	24.78	2.73	ZrO_2 = 1.65
10	Grout[8]	1.648	8.63	12.96	20.72	4.34	
11	Grout[8]	1.639	.64	17.60	18.18	1.50	
12	Jakob[9]	1.625	5.03	15.84	20.37	1.95	
13	Jakob[9]	1.643	4.03	16.26	19.89	3.16	
14	Jakob[9]	1.634	4.08	16.85	20.52	2.71	
15	von Eckermann[10]	1.631	2.01	21.54	23.35	2.74	
16	Karvano[11]	1.633	3.28	16.38	19.33	2.45	
17	Kranck[12]	1.632	9.12	21.62	29.83	tr	
18	Deer[13]	1.656	3.22	19.94	22.84	3.48	
19	Deer[13]	1.652	2.48	19.07	21.30	3.63	
20	Deer[13]	1.650	2.90	18.30	20.91	3.99	
21	Tsuboi[14]	1.657	4.49	15.00	19.04	3.29	MnO = 0.52
22	Tsuboi[14]	1.656	2.07	18.97	20.83	2.62	MnO = 0.33
23	Tsuboi[14]	1.655	1.00	20.09	21.99	2.52	MnO = 0.51
24	Tsuboi[14]	1.665	3.37	20.15	23.18	2.77	MnO = 0.43
25	Tsuboi[14]	1.650	1.00	19.23	20.13	3.30	MnO = 0.13
26	Tsuboi[15]	1.673	2.42	25.60	27.78	2.28	MnO = 1.66
27	Tsuboi[15]	1.670	2.10	26.80	28.69	3.33	MnO = 0.50
28	Tsuboi[15]	1.672	3.02	26.02	28.74	2.74	MnO = 0.84
29	Tsuboi[3]	1.638	0.68	16.88	17.49	2.65	MnO = 0.35
30	Tsuboi[3]	1.672	1.05	26.34	27.28	3.79	MnO = 0.58
31	Tsuboi[3]	1.661	0.87	20.88	21.66	3.53	MnO = 0.63
32	Tsuboi[3]	1.657	0.71	20.80	21.44	3.20	MnO = 0.80
33	Tsuboi[3]	1.675	1.86	26.17	27.84	3.64	MnO = 0.67
34	Tsuboi[3]	1.651	0.87	21.10	21.88	3.29	MnO = 0.48
35	Tsuboi[3]	1.646	0.27	19.46	19.70	4.07	MnO = 0.16
36	Tsuboi[3]	1.658	0.76	18.39	21.48	4.68	MnO = 0.20
37	Tsuboi[3]	1.661	3.00	18.83	21.53	3.15	MnO = 0.34
38	Tsuboi[3]	1.660	0.77	21.42	22.11	3.28	MnO = 0.45
39	Tsuboi[3]	1.660	2.95	18.87	21.53	3.07	MnO = 0.35
40	Tsuboi[3]	1.649	0.69	18.11	18.73	2.99	
41	Chapman[16]	1.656	nil	15.52	15.52	5.22	
42	Chapman[16]	1.665	2.33	20.88	22.98	4.17	
43	Chapman[16]	1.672	8.00	23.54	30.74	2.94	
44	Hall†	1.619	3.33	6.73	9.73	1.66	
45	Hall	1.632	2.59	14.40	16.73	2.95	
46	Hall†	1.637	2.79	14.26	16.77	3.90	
47	Hall†	1.639	2.78	14.84	17.34	2.20	
48	Hall	1.642	1.62	16.02	17.48	4.59	
49	Hall	1.642	2.73	17.08	19.54	3.74	
50	Hall	1.644	3.46	16.92	20.04	4.21	
51	Hall	1.646	1.42	19.27	20.55	4.99	
52	Hall†	1.647	3.16	20.34	23.18	4.01	
53	Hall	1.648	1.83	21.54	23.19	3.52	
54	Hall	1.648	2.39	20.99	23.14	4.31	
55	Hall	1.649	1.51	20.53	21.89	5.27	
56	Hall†	1.651	1.03	20.56	21.49	3.05	
57	Hall	1.651	2.60	19.17	21.51	3.68	
58	Hall†	1.654	3.05	22.06	24.81	5.40	
59	Prider[17]	1.643	2.18	3.73	5.69	8.97	

† Analyst: N. Sahlbom.

amount of titania. This may be expressed in the following way:—

Let x = the amount of Fe present.
y = the amount of Ti present
A = the influence of Fe on the refractive index (γ)
B = the influence of Ti on the refractive index (γ)

The refractive index may then be calculated from the equation

$$xA+yB=\gamma$$

We do not know what exactly is the influence of Fe (either as Fe'' or Fe''') on the refractive index, but we do know the refractive index of such a biotite as Nockolds' siderophyllite which contains practically no titania. This siderophyllite has the same amount of total FeO as biotite No. 55 (Table 1). The value of γ for the siderophyllite is 1.625 and for the biotite No. 55 is 1.649. No. 55 contains 5.27% TiO_2, so that the amount by which 1% of TiO_2 raises the refractive index is:—

$$\frac{1.649-1.625}{5.27}=.0046$$

The correctness of this value may be tested by calculating the refractive indices of various biotites given in Table 1. The line drawn between Nockolds' and Kranck's siderophyllites (Nos. 5 and 17) has been used for reading off the values of the refractive index for the various values of total FeO. The results of the calculations are given below:—

TABLE 2

Biotite	Total FeO	TiO_2	Observed γ	Calculated γ	Error
1	12.35	5.08	1.640	1.640	.000
2	17.93	3.54	1.645	1.636	−.009
7	18.44	2.23	1.640	1.632	−.008
14	20.52	2.71	1.634	1.636	+.002
15	23.35	2.74	1.631	1.640	+.009
16	19.33	2.45	1.633	1.634	+.001
19	21.30	3.63	1.652	1.640	−.012
29	17.49	2.65	1.638	1.634	−.004
32	21.44	3.20	1.657	1.638	−.019
46	16.77	3.90	1.637	1.639	+.002
48	17.48	4.59	1.642	1.643	+.001
54	23.14	4.31	1.648	1.647	−.001
57	21.51	3.68	1.651	1.642	−.009
58	24.81	5.40	1.654	1.652	−.002

It will be seen from Table 2 that in many cases the calculated value of γ agrees with the observed value of γ within small limits of error, but that at other times the discrepancy is somewhat large. If the value given by Kunitz had been taken, the error in most cases would have been still greater. It is understandable that there should be some differences between the calculated and observed values of γ since, in the first place, the data upon which the calculation is founded are rather scanty, and in the second place no allowance is made for the presence of Fe_2O_3, Ti_2O_3, MnO, etc., in the biotites. Grout (8) believes that many authors quote too low values for the refractive indices of their biotites. He himself was dealing with biotites several of which contained quite appreciable amounts of Fe_2O_3 and which, therefore, could not be compared with biotites from other areas containing less Fe_2O_3.

In conclusion it may be said that no sure information can be obtained as to the chemical composition of a biotite from its refractive index alone, since a biotite which is high in iron and low in titania may have the same refractive index as one which is low in iron and high in titania. Much work remains to be done upon the analyses of the end members of the biotite series together with careful determinations of their refractive indices.

ACKNOWLEDGMENT

The work contained in this paper was carried out in the Department of Mineralogy and Petrology, Cambridge, England. The author wishes to thank Professor C. E. Tilley for helpful discussions and advice during the course of the work, Dr. W. A. Wooster for suggestions on the calculation of the refractive indices and Dr. S. R. Nockolds for communicating four biotite analyses which were unpublished up to the time of writing. A grant from the Royal Society of London to defray the cost of six biotite analyses is also gratefully acknowledged.

REFERENCES

(1) WINCHELL, A. N., (*a*) Studies in the mica group: *Am. Jour. Sci.*, **9**, 309, 415 (1925). (*b*) The biotite system: *Am. Mineral.*, **20**, 773–779 (1935).

(2) LARSEN, E. S., IRVING, J., GONYER, F. A., and LARSEN, E. S., 3RD., Petrologic results of a study of the minerals from the Tertiary volcanic rocks of the San Juan Region, Colorado: *Am. Mineral.*, **22**, 902–903 (1937).

(3) TSUBOI, S., Petrological notes: *Japan. Jour. Geol., Geogr.*, **15**, 126–127 (1938).

(4) KUNITZ, W., *Zeits. Krist.*, **70**, 508 (1929).

(5) KÔZU, S., and YOSHIKI, B., Thermo-optic studies of anomite-basaltic hornblende-quartz-andesite in association with biotite-common hornblende-quartz-andesite, which together form the volcano Sambé, Japan: *Sci. Reports Tôhoku Imp. University, Ser. III*, **3**, 177–193 (1929).

(6) Jakob, J., and Parga-Pondal, I., Über die Rolle des Titans in den Phlogopiten: *Zeits. Krist.*, **82,** 271–284 (1932).

(7) Nockolds, S. R., and Richey, J. E., Replacement veins in the Mourne Mountains granites, N. Ireland: *Am. Jour. Sci.*, **237,** 38 (1939).

(8) Grout, F. F., Notes on biotite: *Am. Mineral.*, **9,** 159 (1924).

(9) Jakob, J., *Zeits. Krist.*, **79,** 373 (1931).

(10) Eckermann, H. von., Die Glimmermineralien im Mansjo-Kalkkontakt: *Tschmer. Min. Petr. Mitt.*, **38,** 277–287, (1925).

(11) Karvano, Y., Chemical studies of the orbicular rock from Minedna-Yama: *Proc. Imp. Acad. Tokyo*, **9,** 609–612 (1933).

(12) Kranck, E. H., A beryl-bearing pegmatite from Uuku in Carelia: *Bull. Com. Géol. Finlande*, No. **85,** 70–77 (1929).

(13) Deer, W. A., The composition and paragenesis of the biotites of the Carsphairn igneous complex: *Min. Mag.*, **24,** No. 156, 495–502 (1937).

(14) Tsuboi, S., Petrological notes: *Jap. Jour. Geol., Geogr.*, **12,** 112–113 (1935).

(15) Tsuboi, S., Petrological notes: *Jap. Jour. Geol., Geogr.*, **13,** 334–335 (1936).

(16) Chapman, R. W., and Williams, C. R., Evolution of the White Mountain series: *Am. Mineral.*, **20,** 502 (1935).

(17) Prider, R. T., Some minerals from the leucite-rich rocks of the West Kimberley area, Western Australia: *Min. Mag.*, **25,** 373–387 (1939).

(18) Lewis, H. C., On siderophyllite, a new mineral: *Proc. Acad. Sci. Philadelphia*, 254–255 **(1880).**

(19) Harada, Z., Chemische Analysenresultate von japanischen Mineralien: *Jour. Fac. Sci. Imp. Univ. Hokkaido*, Ser. 4, **3,** 319 (1936).

(20) Kunitz, W., Die Rolle des Titans und Zirkoniums in dem gesteinsbildenen Silikaten: *N. Jahrb. Min., B. Bd.* **70,** 385–466 (1936).

NOTES ON SOME MARIE BYRD LAND ROCKS

Duncan Stewart, Jr.,
Carleton College, Northfield, Minnesota.

Abstract

A petrographic qualitative study has been made of forty-four metamorphic and three sedimentary rocks of the Edsel Ford Ranges, Marie Byrd Land, Antarctica, and comparisons made between these rocks and those examined from other Antarctic lands.

Introduction

A brief review of the literature pertaining to the petrography of the Pacific Antarctic reveals that thirty-four reports have been published which describe rocks collected between the meridians 180° and 90°W., and between the meridians 80° and 50°W.[1] Little attention has been devoted to the study of the metamorphic rocks in the areas delimited by those meridians, and virtually nothing is known about the rocks included between those two sectors. A brief report on the petrography of the metamorphics collected at Scott's Nunataks, King Edward VII Land, has been made by Schetelig.[2] The author[3] has published a report on quantitative microscopical analyses of some schists collected in the Queen Maud Mountains, Marie Byrd Land, and Wade[4] has made a statement about the metamorphic rocks of the Edsel Ford Ranges, Marie Byrd Land.

A number of metamorphic rocks of South Victoria Land have been described by Mawson,[5] Prior,[6] Schetelig,[7] Smith,[8,9] Stewart,[10] and Woolnough.[11] Probably the most noteworthy report on Antarctic metamorphic rocks is the monograph by Stillwell,[12] treating of Adelie Land specimens. Three other reports of the Australasian Antarctic Expedition should be noted, namely, by Coulson,[13] Stillwell,[14] and Tilley.[15]

---

[1] Stewart, Duncan, Jr., Petrography of rocks from the Pacific Antarctic: *Proc. Sixth Pac. Sci. Cong.*, 1939, 741–746 (1940).

[2] Schetelig, J., Report on the rock specimens collected on Roald Amundsen's South Pole Expedition: *Videnskapsselskapets Skrifter, I, Mat. -naturv Klasse*, No. **4,** 21–25, Christiania (1915).

[3] Stewart, Duncan, Jr., A contribution to Antarctic petrography: *Journ. Geol.*, **42,** No. 5, 546–548 (1934).

[4] Wade, F. A., Petrologic and structural relations of the Edsel Ford Range, Marie Byrd Land, to other Antarctic mountains: *Bull. Geol. Soc. Am.*, **48,** 1390–1391 (1937).

[5] Mawson, D., Petrology of rock collections from the mainland of South Victoria Land. Contributions to the paleontology and petrology of South Victoria Land: British Antarctic Expedition, 1907–9, under the command of Sir. E. H. Shackleton, *Reports of the Scientific Investigations, Geology,* **II,** Part XIII, 230–232 (1916).

[6] Prior, G. T., Report on the rock specimens collected during the 'Discovery' Antarctic Expedition, 1901–04: National Antarctic Expedition, 1901-1904, Natural History, Vol. I. *Geology* (Field-Geology: Petrography), Part **II,** 124–125 (1907).

[7] Schetelig, J., *op. cit.*, 11–12.

Acknowledgments

This study has been carried on at the request of Dr. F. Alton Wade who collected the specimens in the Edsel Ford Ranges. Dr. Wade has kindly loaned the author forty thin sections of the metamorphic specimens and three of the sedimentary rocks. He has donated to the University of Michigan Antarctic collections a suite of fifty-one rocks, making the total number of pieces, from various parts of the Antarctic, in the collections at the present time, three hundred and eighty-one.

Characteristics of the Rocks

The metamorphic rocks, of which qualitative microscopical analyses of forty-four thin sections are recorded in Table 1, were collected in the Edsel Ford Ranges, Marie Byrd Land (Fig. 1). The two sandstones examined are from Mt. 73, Claude Swanson Mountains, and correspond mineralogically to the sandstones of the Beacon formation of South Victoria Land.[16] The oolitic limestone was collected at Mt. Corey, and is one of two specimens labeled "carbonate pisolites." The size of a few particles indicates that the diameters are less than two millimeters,

---

[8] Smith, W. Campbell, and Debenham, F., The metamorphic rocks of the McMurdo Sound region. The metamorphic rocks of South Victoria Land: British Antarctic ("Terra Nova") Expedition, 1910, Natural History Report, *Geology*, **I**, No. 5a, 131–144 (1912).

[9] Smith, W. Campbell, and Priestley, R. E., The metamorphic rocks of the Terra Nova Bay region: *Ibid.*, No. **5b**, 145–165 (1921).

[10] Stewart, Duncan, Jr., The petrography of some rocks from South Victoria Land: *Proc. Am. Philosophical Soc.*, **74**, No. 4, 309–310 (1934).

[11] Woolnough, W. G., Petrological notes on some erratics collected at Cape Royds. Contributions to the paleontology and petrology of South Victoria Land: British Antarctic Expedition, 1907–9, under the command of Sir. E. H. Shackleton, *Reports of the Scientific Investigations*, *Geology*, **II**, Part XI, 183–186 (1916).

[12] Stillwell, F. L., The metamorphic rocks of Adelie Land: Australasian Antarctic Expedition, 1911–1914, *Scientific Reports*, Series A, **III**, Part I, 1–230 (1918).

[13] Coulson, A. L., Magnetite garnet rocks from the moraines, Cape Denison, Adelie Land: *Ibid.*, Part **5**, 281–305 (1925).

[14] Stillwell, F. L., Amphibolites and related rocks from the moraines, Cape Denison, Adelie Land: *Ibid.*, Part **4**, 259–280 (1923).

[15] Tilley, C. E., Metamorphic limestones of Commonwealth Bay, Adelie Land: *Ibid.*, Part **2**, 231–244 (1923).

[16] Stewart, Duncan, Jr., The petrography of the Beacon Sandstone of South Victoria Land: *Am. Mineral.*, **19**, 351–359 (1934).

therefore oolitic is the preferred term. Skeats[17] has reported on an oolitic limestone erratic from the Cloudmaker, Beardmore Glacier, South Victoria Land.

Quartz showing undulatory extinction is present in all nine of the gneisses examined. Zoning of the acid plagioclases is recorded in eight sections and micrographic intergrowths are seen in five of the gneisses.

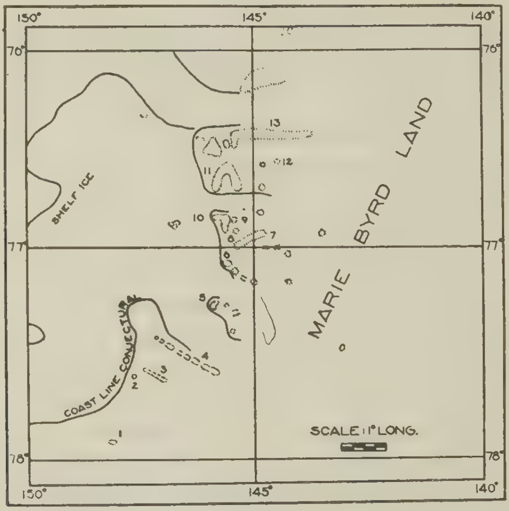

FIG. 1. Sketch map of the Edsel Ford Ranges, Marie Byrd Land. (after Chart No. 5412, 1st ed., Sept., 1939, published at the Hydrographic Office, U. S. Navy, and F. Alton Wade).

1. Mt. Grace McKinley.
2. Mt. 5.
3. Garland Hershey Ridge.
4. Haines Mts.
5. Donald Woodward Mt.
6. Mt. Rea.
7. Claude Swanson Mts.
8. Mt. 73, Claude Swanson Mts.
9. Mt. Stancliffe.
10. Mt. Saunders.
11. Chester Mts.
12. Mt. Corey.
13. Raymond Fosdick Mts.

In one section (155x) there is evidence of antiperthite. Tilley[18] has reported the occurrence of antiperthite in a coarse pegmatitic quartz diorite, in an acid member of the charnockite series, in three garnet orthogranulites and in two specimens of igneous gneiss erratics from Proclamation Island, Enderby Land. He[19] has reported antiperthitic plagioclase as occurring in some of the paragneisses and granite and granodiorite gneisses from Cape Bruce, MacRobertson Land. The author[20] has reported the occurrence of antiperthite in three igneous and one metamorphic erratics from the Terra Nova Bay region, South Victoria Land. Bent plagioclase twinning lamellae are seen in three sections of gneisses from the Edsel Ford Ranges. Dark dust-like inclusions which are probably magnetite are noted in the apatites of two slides. This same feature is seen in the sections of intrusives from Marie Byrd Land.

---

[17] Skeats, E. W., Report on the petrology of some limestones from the Antarctic. Contributions to the paleontology and petrology of South Victoria Land: British Antarctic Expedition, 1907–9, under the command of Sir E. H. Shackleton, *Reports of the Scientific Investigations*, *Geology*, **II**, Part XII, 191–192 (1916).

[18] Tilley, C. E., Rocks from Enderby Land: B.A.N.Z. Antarctic Research Expedition, 1929–1931, under the command of Sir Douglas Mawson, Reports, Series A, **II** (*Geology*), Part **1**, 5, 6, 9, 12 (1937).

Smith's report[21] on para-diopside granulite erratics indicates that there is similarity in mineral composition between the Terra Nova Bay, South Victoria Land, specimens and the diopside granulite collected by Wade at Donald Woodward Mt. Walkom[22] has described some pyroxene granulites collected as erratics at Cape Royds, Ross Island, South Victoria Land, that show similarity to the granulite collected by Wade.

Discussion

Wade[23] states:

> Of the metamorphic rocks observed and studied the only one which might be considered to represent the basement complex of East Antarctica is the granite gneiss of the Raymond Fosdick Mountains. The metamorphosed sedimentary series has not undergone such intense alteration as the basement gneiss, and no minerals characteristic of high temperature metamorphism were noted in the thin sections examined. Recrystallization varies in intensity, and cataclastic texture is exceptional.

After a review of the literature pertaining to the petrography of Antarctic metamorphic rocks and an examination of Wade's and other thin sections of Antarctic metamorphics, it may be said that none of the rocks collected by him show East Antarctica basement complex affinities. The gneisses from the Raymond Fosdick Mountains are relatively simple in mineralogical composition and exhibit some characteristics under the microscope of the intrusives of the Edsel Ford Ranges, such as zoned feldspar and micrographic intergrowths, and lack features commonly referred to as characteristic of the metamorphosed basement rocks.

---

[19] Tilley, C. E., Rocks from MacRobertson Land, Antarctica: *Ibid.*, Part **2,** 20, 22 (1937).

[20] Stewart, Duncan, Jr., Petrography of some rocks from South Victoria Land: *Am. Mineral.*, **24,** 158 (1939).

[21] Smith, W. Campbell and Priestley, R. E., *op. cit.*, 156–158.

[22] Walkom, A. B., Report on the pyroxene granulites collected by the British Antarctic Expedition, 1907–1909. Contributions to the paleontology and petrology of South Victoria Land: British Antarctic Expedition, 1907–9, under the command of Sir E. H. Shackleton, *Reports of the Scientific Investigations, Geology,* **II,** 161–168 (1916).

[23] Wade, F. A., *op. cit.*, 1390–1391.

Reference has been made to myrmekite, diablastic structure, micrographic intergrowths and micropegmatite in Antarctic literature. Smith[24] remarks that erratics of pyroxene gneiss, collected at Cape Bernacchi and Marble Point, McMurdo Sound, South Victoria Land, exhibit well-developed myrmekite. He[25] refers, also, to the gneisses of Cape Sastrugi and records that in some types in thin section no signs of metamorphism are apparent, except the development of myrmekite in the plagioclase. The author has noted micrographic intergrowths in a section of muscovite-biotite schist collected by Gould at the base of a cliff two miles east of the foot of Liv Glacier, South Victoria Land. Prior[26] records the fact that in the metamorphics studied by him from South Victoria Land micropegmatite is characteristic of some gneisses. Stillwell[27] states that in a number of the Adelie Land sections diablastic structure is noted. Schetelig[28] notes the presence of myrmekite along the borders of microcline in granite gneiss from Mt. Betty, South Victoria Land. He[29] also records an interesting intergrowth of quartz and bytownite in an amphibolite from Scott's Nunataks, King Edward VII Land. Tilley[30] states that myrmekitic plagioclase is present in three garnet orthogranulites and in three erratics of igneous gneisses from Proclamation Island, Enderby Land. He[31] records myrmekitic structures in the granite and granodiorite gneisses of MacRobertson Land.

In none of the reports on the basement rocks of East Antarctica is the zoning of plagioclase in the metamorphics mentioned. As previously stated, eight of the nine sections of gneisses examined from Marie Byrd Land contain zoned plagioclase. The author has noted zoned plagioclase in one specimen of oligoclase-biotite gneiss, collected by Gould, at O'Brien Peak, Queen Maud Mountains, South Victoria Land. Schetelig[32] does record the presence of indistinct zoning of the plagioclase in an amphibolite from Scott's Nunataks, King Edward VII Land. A study by the author of the metamorphics collected by Gould at Supporting Party Mountain, Queen Maud Mountains, Marie Byrd Land, revealed the fact that micrographic intergrowths were present in only one of the eleven thin sections of the seven metamorphic rocks examined and that none of the sections exhibited zoned plagioclase. Considering the careful investigations that have been carried on and the noticeable lack of a mention of zoned plagioclase in Antarctic metamorphic rocks, this structure might well be considered as a characteristic of some of the gneisses of the Edsel Ford Ranges.

---

[24] Smith, W. Campbell, and Debenham, F., *op. cit.*, 143.

[25] *Ibid.*, 150.

[26] Prior, G. T., *op. cit.*, 124–125.

[27] Stillwell, F. L., *op. cit.*, 25.

[28] Schetelig, J., *op. cit.*, 11.

[29] *Ibid.*, 21–22.

[30] Tilley, C. E., *op. cit.*, 9, 12.

[31] Tilley, C. E., *op. cit.*, 22.

[32] Schetelig, J., *op. cit.*, 21.

In the rocks collected farther south in Marie Byrd Land, at Supporting Party Mountain, such minerals as garnet and sillimanite were noted. The Adelie Land metamorphics are apparently characterized by such minerals as cordierite, garnet, hypersthene, kyanite, scapolite and sillimanite; the South Victoria Land rocks collected in the McMurdo Sound region, by andalusite, cordierite, garnet and sillimanite, and the metamorphics of Enderby and MacRobertson Lands are characterized by similar minerals. These minerals, as far as is known, are not characteristic of the rocks of the Edsel Ford Ranges.

From what data is available it appears that the majority of the metamorphics examined from the Edsel Ford Ranges were originally sedimentary rocks, with the exception of the gneisses which show in many instances preserved igneous characteristics.

CONCLUSIONS

A review of the literature and a study of thin sections of rocks from Marie Byrd Land and other Antarctic lands indicates that the metamorphic types from the Edsel Ford Ranges are quite different mineralogically from the metamorphic basement rocks of certain other parts of the Continent and must be considered of an age other than pre-Cambrian. Further field data must be supplied before the age of the metamorphics can be ascertained.

TABLE 1. MINERALOGICAL COMPOSITION OF SOME METAMORPHIC ROCKS FROM MARIE BYRD LAND

Mineral	Specimen																							
	119	155	155x	175	186	259	265A	265B	177	90	92	93	94	156	163	89	167	607	216B	37	391	40	16	38
Quartz	p	p	p	p	p	p	p	p	p	p	p	p	p	p	p	p	p	p	p	p	p	p	p	p
Cryptocrystalline quartz	–	–	–	–	–	–	–	–	–	–	–	–	–	–	–	–	–	–	–	p	–	–	–	–
Feldspar (undet.)	–	–	–	–	–	–	–	–	–	–	–	–	–	–	–	–	–	–	–	–	–	–	–	–
Orthoclase	–	–	–	–	–	p	–	–	–	–	–	–	–	–	–	–	–	–	–	–	–	–	–	–
Microperthite	–	–	p	p	–	–	–	–	–	–	–	–	–	–	–	–	–	–	–	–	–	p	–	–
Acid plagioclase	–	–	–	p	–	–	–	–	–	–	–	p	–	–	–	–	p	p	p	–	–	p	p	p
Oligoclase	–	p	p	–	–	p	p	p	p	p	–	–	–	–	–	–	–	–	–	–	–	–	–	–
Oligoclase-andesine	p	–	–	–	p	–	–	–	–	–	–	–	–	–	–	–	–	–	–	–	–	–	–	–
Andesine	–	–	–	–	–	–	–	–	–	–	–	–	–	–	–	–	–	–	–	–	–	–	–	–
Bytownite	–	–	–	–	–	–	–	–	–	–	–	–	–	–	–	–	–	–	–	–	–	–	–	–
Diopside	–	–	–	–	–	–	–	–	–	–	–	–	–	–	–	–	–	–	–	–	–	–	–	–
Green hornblende	–	–	–	–	–	–	–	–	–	–	–	–	–	–	–	–	–	–	–	–	–	–	–	–
Biotite	p	p	p	p	p	p	p	p	p	p	p	p	p	p	p	p	p	p	p	–	–	–	–	–
Chlorite	–	–	p	p	–	p	p	p	–	p	–	p	–	p	–	–	–	p	–	–	–	–	–	p
Muscovite	–	p	p	p	–	p	p	p	p	p	p	p	p	p	–	p	p	p	p	p	p	–	p	p
Apatite	p	p	p	p	p	p	p	p	p	p	p	p	p	p	p	p	p	p	p	p	p	p	p	p
Zircon	p	p	p	p	p	p	p	p	p	p	p	p	p	p	p	p	p	p	p	p	–	p	p	p
Tourmaline	–	–	–	–	–	–	p	–	–	p	p	p	p	–	p	p	–	p	p	p	p	p	p	p
Yellow rutile	–	–	–	–	–	p	p	p	p	–	–	–	–	–	p	–	–	–	–	p	–	–	p	–
Pistacite	–	–	–	–	–	–	–	–	–	–	–	–	–	–	–	–	–	–	–	?	–	–	?	–
Zoisite	–	–	–	–	–	–	–	–	–	–	–	–	–	–	–	–	–	–	–	–	–	–	–	–
Sphene	–	–	–	p	–	–	–	–	–	–	–	–	–	–	–	–	–	p	p	–	p	–	–	p
Fluorite	–	p	p	–	–	–	–	–	–	–	–	–	–	–	–	–	–	–	–	–	–	–	–	–
Rutile (?) needles	–	p	p	–	–	–	–	–	–	p	–	–	–	–	p	–	p	–	–	p	–	p	p	p
Magnetite	–	p	p	p	p	p	p	p	p	p	p	p	p	–	p	p	–	p	p	p	p	p	p	p
Ilmenite	–	–	–	–	–	–	–	–	–	–	–	–	–	–	–	–	–	–	–	–	–	–	p	–
Pyrite	–	–	–	–	p	–	p	p	–	–	–	–	–	–	–	p	–	–	p	–	–	–	p	–
Hematite	–	p	p	p	p	p	p	p	p	p	–	p	–	–	p	p	–	–	p	–	p	p	p	p
Limonite	–	p	p	p	p	–	p	–	p	p	p	p	p	–	p	p	–	–	p	p	p	p	p	–
Leucoxene	–	–	–	–	–	–	–	–	p	p	–	–	–	–	p	–	–	–	–	p	p	p	p	p
Calcite	–	–	–	–	–	–	–	–	–	p	–	–	–	–	–	–	–	–	–	p	p	p	p	p
Sericite	p	p	p	p	p	p	p	p	p	p	–	–	–	–	–	–	p	p	p	p	–	p	p	p
Kaolin	–	p	p	p	p	p	p	–	p	–	–	–	–	–	–	–	p	p	–	–	–	–	–	–

p = present in thin section.

119. Biotite gneiss. Raymond Fosdick Mts.
155. Biotite gneiss. Erratic Mt. Rea.
155x. Biotite gneiss. Erratic. Mt. Rea.
175. Biotite gneiss. Raymond Fosdick Mts.
186. Biotite gneiss. Raymond Fosdick Mts.
259. Biotite gneiss. Raymond Fosdick Mts.
265A. Biotite gneiss. Raymond Fosdick Mts.
265B. Biotite gneiss. Raymond Fosdick Mts.
177. Muscovite-biotite gneiss. Chester Mts.
90. Biotite schist. Mt. Rea.
92. Biotite schist. Mt. Rea.
93. Biotite schist. Mt. Rea.
94. Biotite schist. Mt. Rea.
156. Biotite schist. Mt. Rea.
163. Biotite schist. Donald Woodward Mt.
89. Biotite-muscovite schist. Mt. Rea.
167. Muscovite-biotite schist. Mt. Rea.
607. Muscovite-biotite schist. Mt. Grace McKinley.
216B. Quartz schist. Mt. 73, Claude Swanson Mts.
37. Limonitic quartz schist. Garland Hershey Ridge.
391. Calcareous quartz schist. Mt. Corey.
40. Sericite-quartz schist. Haines Mts.
16. Calcareous sericite-quartz schist. Haines Mts.
38. Calcareous sericite-quartz schist. Haines Mts.

TABLE 1 (*Continued*). MINERALOGICAL COMPOSITION OF SOME METAMORPHIC ROCKS FROM MARIE BYRD LAND

Mineral	Specimen																			
	102	109	219	17	34	189	52	64	105	36	215a	215b	230G	39	288	152	161	181	230A	168
Quartz	p	p	p	p	p	p	p	p	p	p	p	p	p	p	p	p	p	p	p	p
Cryptocrystalline quartz	–	–	–	–	p	–	–	–	–	–	–	–	–	–	p	–	–	p	p	–
Feldspar (undet.)	–	–	–	–	–	–	–	p	–	–	–	–	–	–	–	–	–	–	–	–
Orthoclase	p	–	p	–	–	–	p	–	–	–	–	–	–	–	p	–	–	p	–	–
Microperthite	–	–	–	–	–	–	–	–	–	–	–	–	–	–	–	–	–	–	–	–
Acid plagioclase	p	p	p	–	p	–	–	–	–	–	–	–	–	–	p	–	p	p	p	–
Oligoclase	–	–	–	–	–	–	–	–	–	–	–	–	–	–	–	–	–	–	–	–
Oligoclase-andesine	–	–	–	–	–	–	–	–	–	–	–	–	–	–	–	–	–	–	–	–
Andesine	–	–	–	–	–	–	–	–	–	–	–	–	–	–	–	–	–	–	–	?
Bytownite	–	–	–	–	–	?	–	–	–	–	–	–	–	–	–	–	–	–	–	–
Diopside	–	–	–	–	–	–	–	–	–	–	–	–	–	–	–	–	–	–	–	p
Green hornblende	–	–	–	–	–	p	–	–	–	–	–	–	–	–	–	p	–	–	–	–
Biotite	–	–	–	–	–	p	–	–	–	–	–	–	–	–	p	–	p	p	–	–
Chlorite	–	–	p	p	–	–	p	p	–	p	p	p	p	p	p	p	p	p	p	p
Muscovite	p	p	p	p	p	–	–	–	–	–	–	–	–	p	p	p	–	p	p	–
Apatite	p	p	p	p	p	p	–	p	p	–	–	–	–	p	p	p	p	p	p	–
Zircon	p	p	p	–	p	p	–	–	p	–	–	–	–	–	p	p	p	p	p	–
Tourmaline	p	p	p	–	p	–	–	p	–	–	–	–	–	p	p	–	–	p	p	–
Yellow rutile	?	–	–	?	p	–	–	?	?	–	–	–	–	p	–	–	–	p	p	–
Pistacite	–	–	–	–	–	–	–	–	–	–	–	–	–	?	–	–	–	–	–	–
Zoisite	–	–	–	–	–	–	–	–	–	–	–	–	–	–	–	p	–	–	–	p
Sphene	–	p	p	p	–	–	–	–	–	–	–	–	–	–	–	p	–	–	–	p
Fluorite	–	–	–	–	–	–	–	–	–	–	–	–	–	–	–	–	–	–	–	–
Rutile (?) needles	p	–	–	–	p	–	–	–	–	–	–	–	–	–	p	p	p	p	p	–
Magnetite	p	p	p	p	p	p	p	p	p	p	p	p	p	p	p	p	p	p	p	–
Ilmenite	–	–	–	–	–	–	–	–	–	p	–	–	–	–	–	–	–	–	–	p
Pyrite	–	–	p	p	–	–	–	–	–	–	–	–	–	–	–	–	–	–	–	–
Hematite	p	p	p	p	p	p	p	–	p	–	p	p	–	p	p	p	p	p	p	–
Limonite	p	–	p	p	p	p	p	p	p	p	p	p	p	p	p	p	p	p	p	–
Leucoxene	p	p	p	p	p	–	p	p	p	p	–	–	–	p	p	–	–	p	p	–
Calcite	p	p	p	p	p	–	–	p	p	p	–	–	p	p	–	p	p	p	–	p
Sericite	p	p	p	–	p	p	p	p	p	–	p	p	p	p	–	–	–	p	p	–
Kaolin	–	–	–	–	–	–	–	–	–	–	–	–	–	–	–	–	–	–	–	–

p = present in thin section.

102. Calcareous sericite-quartz schist. Haines Mts.
109. Calcareous sericite-quartz schist. Haines Mts.
219. Calcareous mica-quartz schist. Mt. 73, Claude Swanson Mts.
17. Calcareous muscovite-quartz schist. Haines Mts.
34. Calcareous limonitic quartz schist. Garland Hershey Ridge.
189. Amphibolite schist. Raymond Fosdick Mts.
52. Argillite. Erratic. Mt. Saunders.
64. Argillite. Mt. 5.
105. Calcareous phyllite. Haines Mts.
36. Slate. Garland Hershey Ridge.

215a. Slate Mt. 73, Claude Swanson Mts.
215b. Slate. Mt. 73, Claude Swanson Mts.
230G. Slate. Erratic. Mt. Stancliffe.
39. Calcareous slate. Haines Mts.
288. Quartzitic sandstone. (Slate contact.) Mt. Saunders.
152. Quartzite. Donald Woodward Mt.
161. Quartzite. Donald Woodward Mt.
181. Quartzite. (Slate contact.) Mt. Saunders.
230A. Quartzite. Erratic. Mt. Stancliffe.
168. Diopside granulite. Donald Woodward Mt.

NOTES AND NEWS

THE CHEMICAL COMPOSITION OF GARNET ASSOCIATED WITH CORDIERITE

ROBERT E. FOLINSBEE,
University of Minnesota, Minneapolis, Minnesota.

An analysis of euhedral wine-red crystals of a garnet which occurs north of Great Slave Lake, indicates a close chemical control over mineral associations. The garnet occurs as crystals and crystal aggregates with a maximum diameter of 4 inches, in an injection and assimilation gneiss. The associated minerals are cordierite (of gem quality (1)), sillimanite, green spinel, graphite, biotite, quartz, microcline, andesine, and tourmaline.

TABLE 1. ANALYSIS OF GARNET FROM GREAT SLAVE LAKE, N.W.T., CANADA*

SiO_2	37.53		
Al_2O_3	22.42		
Fe_2O_3	0.74		
FeO	32.53	Molecular Composition	
MgO	5.74	Almandite	74.0
CaO	0.16	Pyrope	24.0
H_2O+	0.10	Grossularite	0.5
H_2O-	0.00	Spessartite	1.5
TiO_2	0.03		
MnO	0.66		
	99.91		

* Analysis by the writer in the rock analysis laboratory at the University of Minnesota, under the supervision of Dr. R. B. Ellestad.

Wright (2) has indicated that almandite is the dominant molecule in garnets from biotite schists. Where the three minerals garnet, biotite, and cordierite are associated (a not unusual case) the range in composition of the garnets entering into such an association is limited. These garnets range from 71–78% almandite, from 15–25% pyrope, an average (closely approached by 4 out of the 5 examples) of 2% spessartite, and less than 5% grossularite. (Table 2).

Figure 1 indicates that all garnets within this range of composition are associated with biotite and cordierite, and conversely, that all garnets associated with biotite and cordierite are of this composition.

Within the limited range indicated in Fig. 1 we have the three minerals, garnet, cordierite, and biotite in stable association. These minerals belong

TABLE 2. GARNET FROM CORDIERITE—BIOTITE SCHISTS AND GNEISSES*

	1	2	3	4	5
Almandite	78.3	74.6	71.4	73.4	74.0
Pyrope	14.7	20.3	25.2	17.1	24.0
Spessartite	2.2	2.3	1.6	4.9	1.5
Grossularite	3.8	2.8	1.8	4.6	0.5
Andradite	1.0				

1. Cordierite hornfels, *Centralb. Mineral.*, 356 **(1924).**
2. Cordierite schist, *Neues Jahrb. Mineral.*, *Beil. Band* **34,** 136 (1912).
3. Idem 2.
4. Graphite cordierite schist, *Neues Jahrb. Mineral.*, *Referate* 2, 39 **(1922).**
5. Garnet—cordierite—sillimanite—biotite gneiss, Great Slave Lake (this paper).

* The data for Table 2 and Figure 1 were obtained from Wright's paper, (2) pp. 439, 440, 447; with the addition only of the analysis in Table 1.

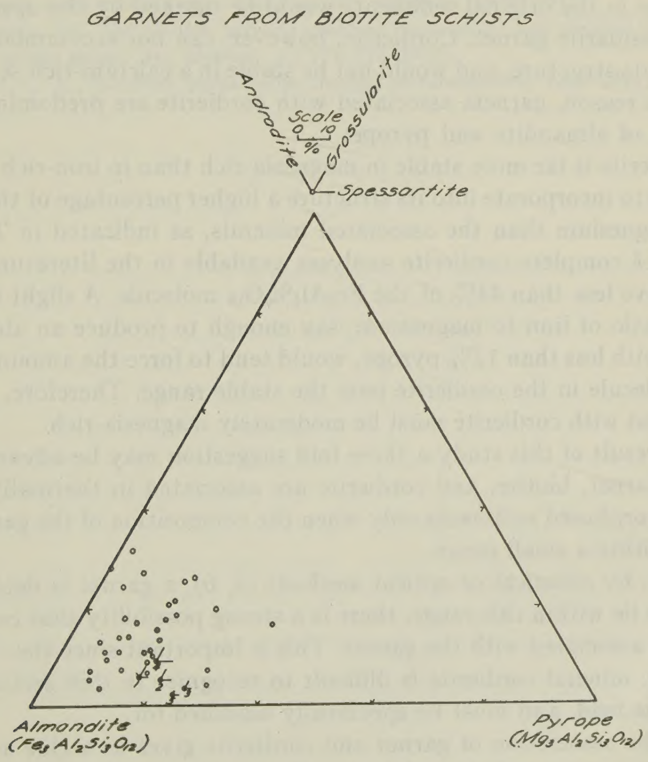

FIG. 1. The limited range in composition of garnets associated with cordierite (Nos. 1–5).

to the ferro-magnesian group in which the Fe-Mg ratio constitutes the chief chemical variable.

For one particular composition of garnet (Number 5, Table 2) the composition of the associated minerals is as follows:

TABLE 3

Garnet	24.0% $Mg_3Al_2Si_3O_{12}$	74.0% $Fe_3Al_2Si_3O_{12}$†
Biotite	39.9% $KMg_3Al\ Si_3O_{10}(OH)_2$	60.1% $KFe_3Al\ Si_3O_{10}(OH_2)$*
Cordierite (3)	61.0% $Mg_2Al_4Si_5O_{18}$	39.0% $Fe_2Al_4Si_5O_{18}$†

* Optical analysis (4).

† Chemical analysis.

An examination of Fig. 1 and Table 3, reveals a logical explanation for the limited range in garnet composition over which garnet, cordierite and biotite are associated. An increase in the vertical component in Fig. 1, (brought about, for example, by an increase in the amount of calcium available in the original sediment) would be marked by the appearance of a grossularite garnet. Cordierite, however, can not accommodate calcium in its structure, and would not be stable in a calcium-rich sediment. For this reason, garnets associated with cordierite are predominantly a mixture of almandite and pyrope.

Cordierite is far more stable in magnesia-rich than in iron-rich schists. It tends to incorporate into its structure a higher percentage of the available magnesium than the associated minerals, as indicated in Table 3. Of the 14 complete cordierite analyses available in the literature, 12 of them have less than 44% of the $Fe_2Al_4Si_5O_{18}$ molecule. A slight increase in the ratio of iron to magnesium, say enough to produce an almandite garnet with less than 12% pyrope, would tend to force the amount of the iron molecule in the cordierite past the stable range. Therefore, garnets associated with cordierite must be moderately magnesia-rich.

As a result of this study a three fold suggestion may be advanced:

(a) Garnet, biotite, and cordierite are associated in thermally metamorphosed sediments only when the composition of the garnet lies within a small range.

(b) If, by chemical or optical methods (5, 6), a garnet is determined to lie within this range, there is a strong possibility that cordierite is associated with the garnet. This is important since the diagnostic mineral cordierite is difficult to recognize in thin section or in the field, and must be specifically searched for.

(c) The association of garnet and cordierite gives us a clue as to the composition of the original sediment. It must have been low in calcium, rich in iron and magnesium (7).

ACKNOWLEDGMENT

The writer takes pleasure in acknowledging the advice and assistance, in the study of this problem, given him by the members of the Department of Geology at the University of Minnesota and by other geologists. In particular he wishes to thank Professor F. F. Grout of the University, Dr. R. B. Ellestad of the rock analysis laboratory at the University of Minnesota, and Drs. A. W. Jolliffe and C. S. Lord of the Geological Survey of Canada.

REFERENCES

(1) FOLINSBEE, Robert E., Gem cordierite from the Great Slave Lake area, N. W. T., Canada: *Am. Mineral.*, **25**, 216 (1940).

(2) WRIGHT, W. I., The composition and occurrence of garnets: *Am. Mineral.*, **23**, 436–443 (1937).

(3) WINCHELL, A. N., Cordierite: *Am. Mineral.*, **22**, 1175–1179 (1937).

(4) GROUT, F. F., Notes on biotite: *Am. Mineral.*, **9**, 159–165 (1929).

(5) FORD, W. E., A study of the relations existing between the chemical, optical and other properties of the garnet group: *Am. Jour. Sci., 4th series*, 33–49 (1915).

(6) FLEISCHER, M., The relation between chemical composition and physical properties in the garnet group: *Am. Mineral.*, **22**, 751–759 (1937).

(7) TILLEY, C. E., Rhombic pyroxene in thermal metamorphism: *Geol. Mag.*, **60**, 411 (1923).

SPESSARTITE IN PEGMATITE AT MOUNT ANTERO, COLORADO

Richard M. Pearl, *University of Colorado, Boulder, Colorado.*

Although more than a dozen papers have appeared since 1887 on the minerals of the Mount Antero region in the Sawatch Range, Colorado, garnet has been mentioned only once.[1] No description of it was published, and it was not included in the most recent article[2] on the locality. After the writer had returned from a nine days' study of the region in July, 1938, two members of his party, Mr. Chester R. Howard and Mr. Jerome Hurianek, found there some attractive garnet crystals. Most of them came from a pegmatite among the steep cliffs about a thousand feet north of the trail, and the same distance above it, in the canyon of Little Browns Creek, which separates Mount Antero from Mount White.

The crystals occur in cavities in dike- and lens-shaped pegmatites in a post-Cretaceous granite stock, which is part of the somewhat earlier (late Mesozoic or Tertiary) Princeton quartz monzonite batholith. The garnet has grown on the typical pegmatite minerals quartz, microcline, and muscovite. The crystals are reddish brown, translucent in spots when fractured, and range in diameter up to 12 millimeters. The trapezohedron is the dominant form, and small dodecahedron faces are also present. On some crystals the trapezohedron is striated parallel to the dodecahedron and shows rhomb-shaped etch figures. A chemical analysis by the writer shows the garnet to be the manganese-aluminum variety, spessartite.

Spessartite is common in the pegmatites of Maine and elsewhere, but this seems to be the first identification of such an occurrence in Colorado. It is found in rhyolite and rhyolite porphyry in a number of places in the state. Interestingly, spessartite is abundant at Ruby Mountain and two other rhyolite hills at Nathrop, directly across the valley of the Arkansas River from Mount Antero. There, in lithophysae in the rock, it occurs as small transparent red crystals of gem quality. The hills, which are dikes intruded into pre-Cambrian granite and gneiss, may be early Tertiary in age, if they can be correlated, as seems likely, with similar bodies in and south of the Tenmile district, near Leadville and Climax. Thus the spessartite may have formed at about the same time in both localities.

---

[1] Over, Edwin, Jr., Further explorations on Mt. Antero: *Rocks and Minerals*, **10,** 28 (1935).

[2] Switzer, George, Granite pegmatites of the Mt. Antero region, Colorado: *Am. Mineral.*, **24,** 791–809 (1939).